

2458-11

Workshop on GNSS Data Application to Low Latitude Ionospheric Research

6 - 17 May 2013

Differential GPS

VAN GRAAS Frank
*Ohio University
School of Electrical Engineering and Computer Science
345 Stocker Center
Athens OH 45701-2979
U.S.A.*

Differential GPS

Fundamentals of GNSS

Workshop on GNSS Data Application to Low Latitude Ionospheric Research

Trieste – Italy, 06-17 May 2013

Prof. Frank van Graas

Ohio University

Overview

- High precision GPS techniques
 - » Relative, differential, wide area differential
 - » Kinematic, surveying, attitude determination
- GPS code and carrier phase measurements
 - » Error sources: Clock and orbit errors, ionospheric and tropospheric propagation delays, multipath, noise, antenna phase and group delays
- Additional implementation considerations

History



First Commercial GPS Receiver

- Installed in DC-3 (1986)
- Differential GPS project to analyze high-accuracy Loran-C (m-level accuracy)

Receiver development (1979 – 1983)

- Hardware: Stanford Telecom, Inc.
- Software: Intermetrics, Inc.
- Integration/nav: MIT Lincoln Lab
- Stand-alone accuracy: 100 m (95%)



Differential/Relative Positioning

- Differential Positioning:
 - » Place one or more reference receivers in known (surveyed) locations and measure the GPS errors
 - » Broadcast the error estimates for each satellite
 - » User applies corrections to its GPS measurements
- Relative Positioning:
 - » Same as differential, except that the corrections are relative to the reference receiver(s)

Example Applications

- Relative GPS
 - » Aircraft carrier landing
 - » Formation flight
 - » Towed hydrographic array
 - » Construction site survey



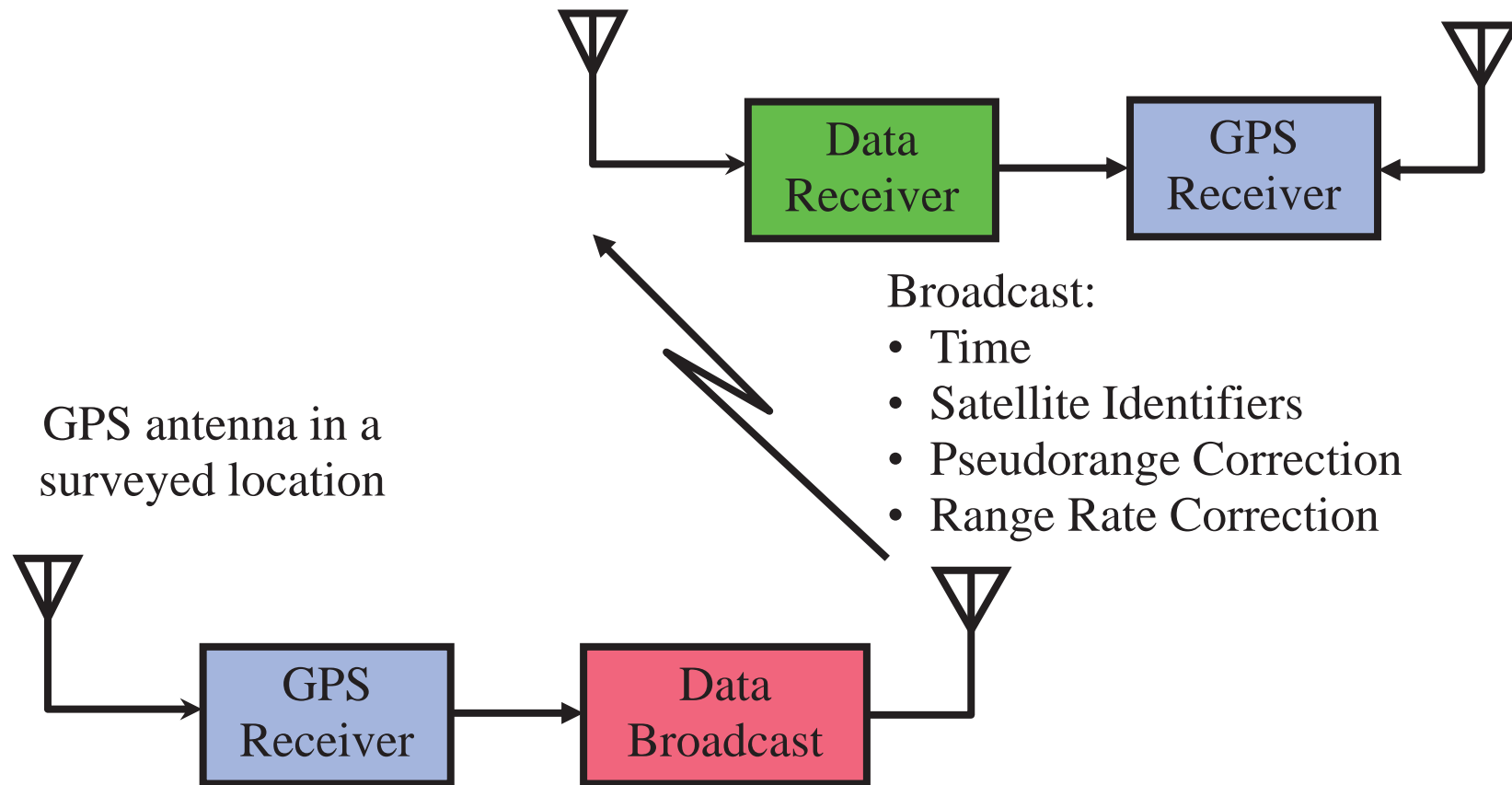
- Differential GPS
 - » Aircraft navigation and precision approach
 - » Georeferencing
 - » Maritime navigation
 - » Surveying



Differential GPS Configurations

- Local-Area DGPS
 - » One correction for each satellite
 - » Examples
 - National Differential GPS (U.S. Coast Guard Network)
 - FAA's Local Area Augmentation System (internationally referred to as Ground Based Augmentation System or GBAS)
 - DoD's Joint Precision Approach and Landing System
- Wide-Area DGPS
 - » Corrections are broken-out into components: orbit, clock, ionosphere, troposphere, so that corrections can be applied as a function of user location
 - » Examples of Space Based Augmentation Systems (SBAS)
 - FAA's Wide-Area Augmentation System (WAAS)
 - EGNOS (Europe), MSAS (Japan), GAGAN (India)

Local Area DGPS Concept



Differential GPS Techniques

- Code-phase: 1 - 2 meter ranging noise
 - » Used for commercial applications where sub-meter accuracy is not required
- Carrier-smoothed code-phase: 0.1 - 0.5 meter ranging noise
 - » Used for most existing high-accuracy systems
- Carrier-phase: less than 0.01 m ranging noise
 - » Most implementations require code-phase for initialization and robustness. Also referred to as kinematic or interferometric GPS
 - » "Standard" for truth reference systems
 - » Involves ambiguity resolution for cm-level accuracy

LAAS Performance Example (L1 and L1/L2)

Code Noise Multipath Algorithm applied to both ground and airborne solutions (L2 only used for carrier)

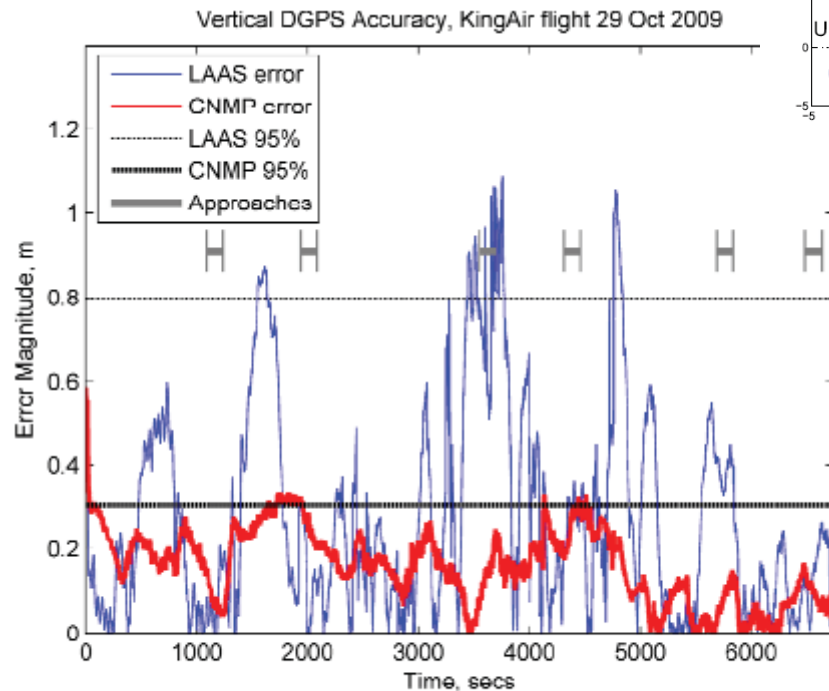
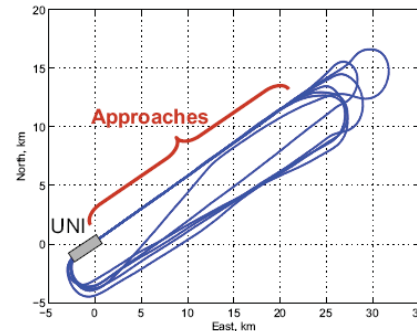
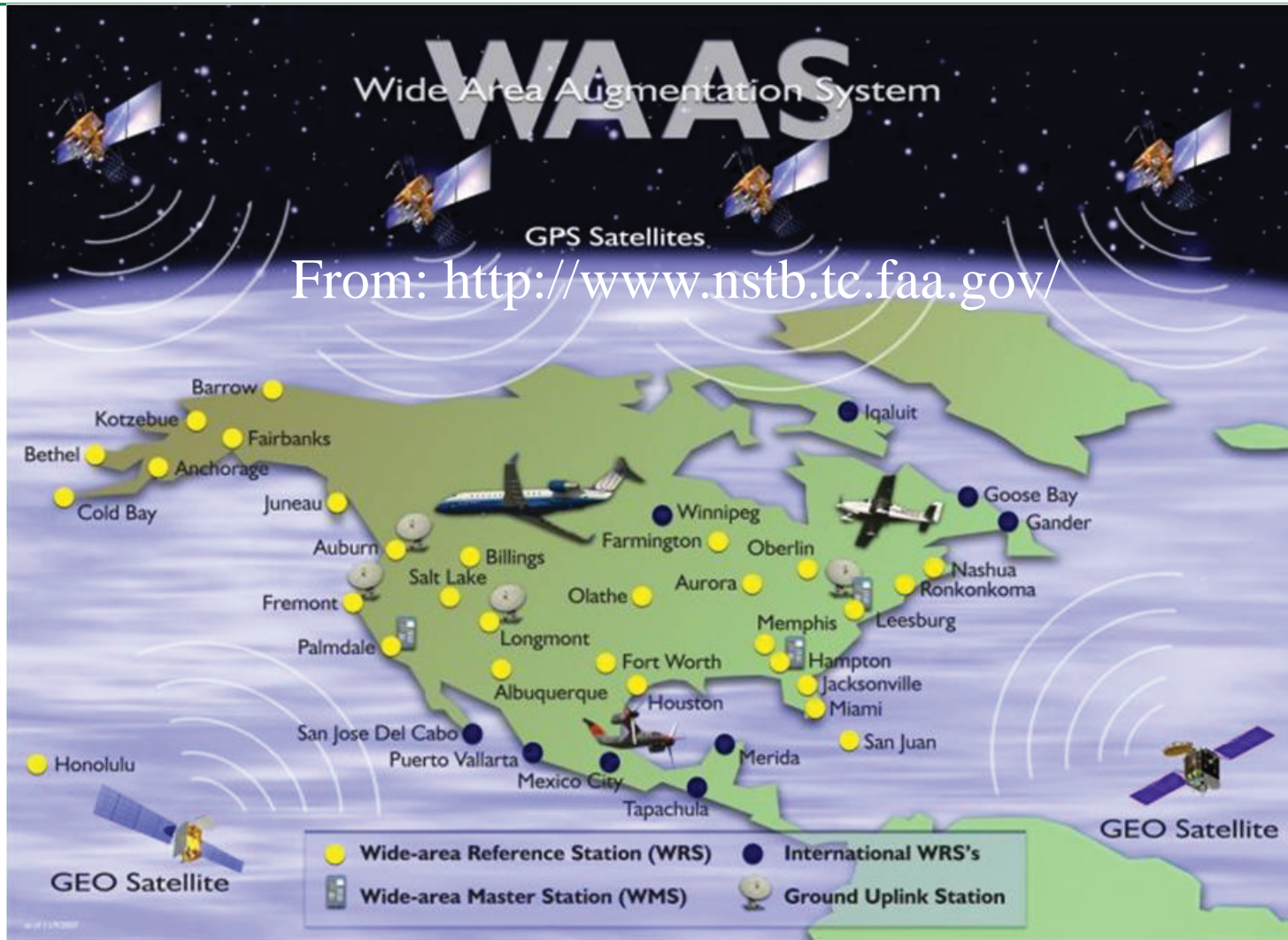


Figure 8: Vertical accuracy and 95% error performance for LAAS and DFD architectures, entire King Air flight test

Table 2: Summary statistics for six approaches (all values in m)

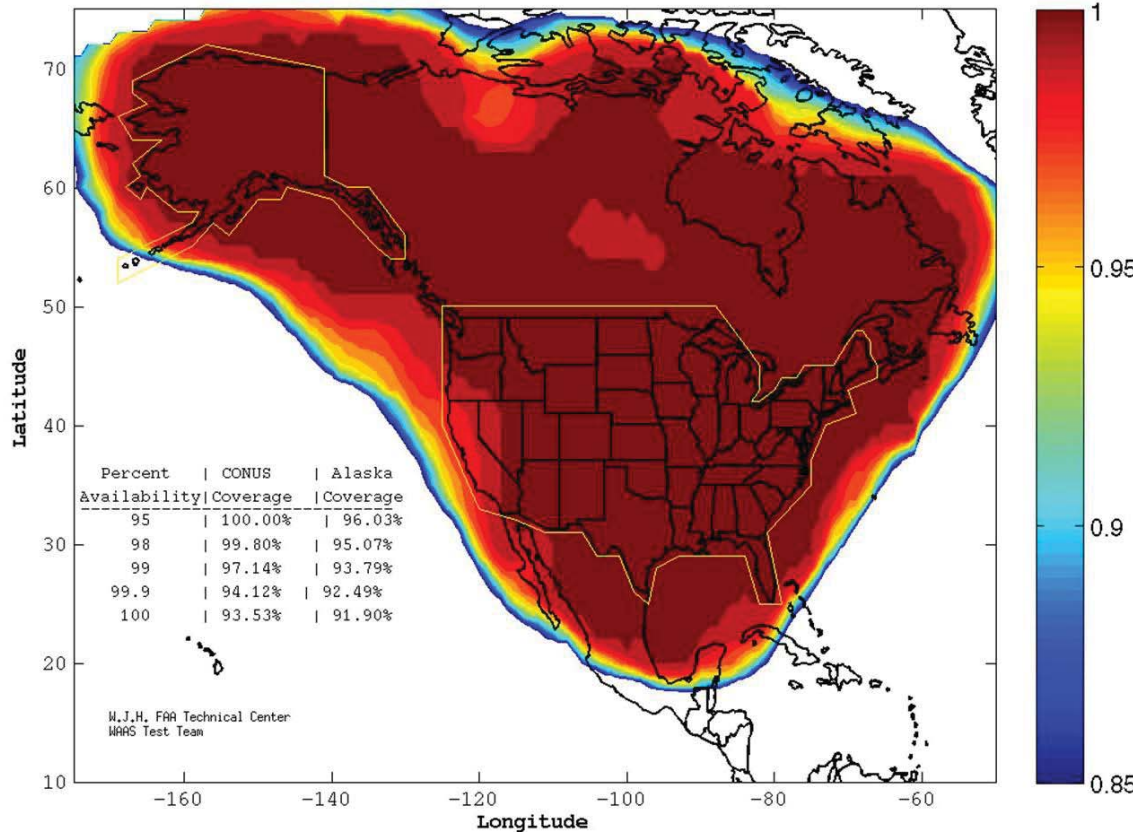
Dimension	Statistic	LAAS	DFD1	Reduction
Vertical	Mean	0.24	0.01	96 %
	Max	1.07	0.32	70 %
	Std Dev	0.13	0.04	69 %
	Rms	0.38	0.18	54 %
	95%	0.56	0.25	65 %
	$ \mu + 2\sigma$	0.59	0.26	56 %
Horizontal	Mean	0.18	0.09	50 %
	Max	0.45	0.16	63 %
	Std Dev	0.13	0.04	69 %
	Rms	0.20	0.10	51 %
	95%	0.28	0.12	60 %
	$ \mu + 2\sigma$	0.30	0.12	59 %

Wide Area Concept



WAAS Coverage for 200-ft Decision Height

WAAS LPV200 Coverage Contours
06/01/12
Week 1690 Day 5



Typical WAAS performance
Horizontal: 1 m (95%)
Vertical: 1.5 m (95%)

Spec: 7.6 m (95%)

Localizer Performance with Vertical Guidance:
LPV-200 Requirements:

95% Accuracy:
Horizontal: 16 m
Vertical: 4 m

Alert limits: 10^{-7} probability of exceeding

Horizontal (HAL): 40 m
Vertical (VAL): 35 m

From: <http://www.nstb.tc.faa.gov/>

GBAS/SBAS

- Performance for GBAS is sub-meter, SBAS 1-2 m
- Key is integrity
 - » WAAS limited by ionospheric disturbances over hundreds of km, resulting in a VPL of 35 m
 - » LAAS limited by local (within 5-10 km range) ionospheric disturbances, resulting in a VPL of 10 m
- Many additional monitors are implemented: e.g. signal deformation, low received signal power, excessive acceleration, code-carrier divergence, interference, cycle slip, long-term noise, ephemeris

VPL: Vertical Protection Level

Overview

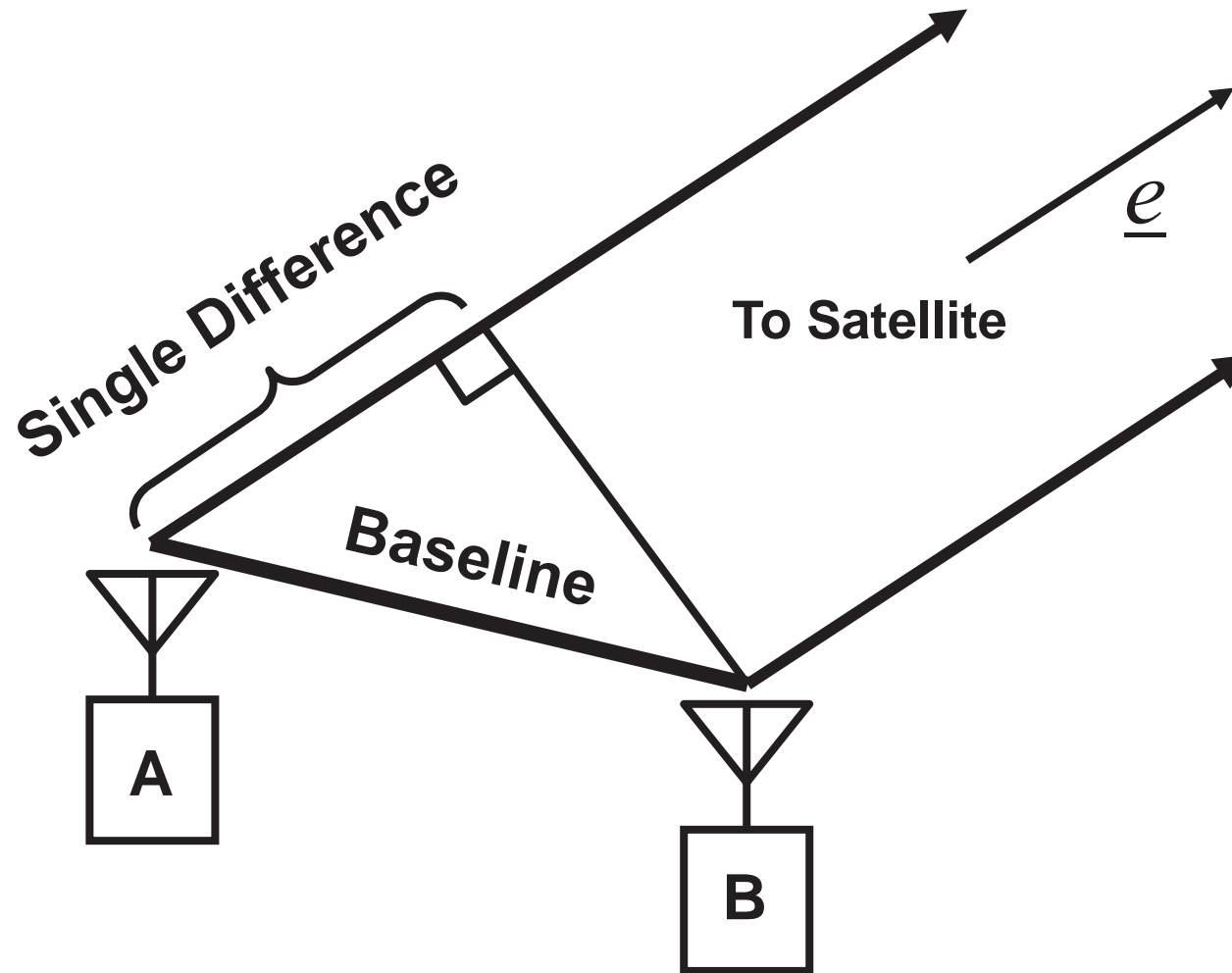
- High precision GPS techniques
 - » Relative, differential, wide area differential
 - » Kinematic, surveying, attitude determination
- GPS code and carrier phase measurements
 - » Error sources: Clock and orbit errors, ionospheric and tropospheric propagation delays, multipath, noise, antenna phase and group delays
- Additional implementation considerations

Kinematic Techniques

- First reported by Dr. Richard Greenspan, et al. in 1982
 - » mm-level accuracy for baselines between 8 and 52 m
- First attitude application in 1983, Burget, Roemerman, Ward
- Speed up of ambiguity resolution in 1984 by Remondi
- Ship attitude determination, Krucynski, et al., 1989
- Post-processed aircraft attitude, Purcell, et al., 1989
- Real-time aircraft attitude and heading, 1991*
- Real-time kinematic autoland (Van Graas, et al.), 1993

* Van Graas, F., Braasch, M. S., "GPS Interferometric Attitude and Heading Determination: Flight Test Results," Proceedings of the 47th Annual Meeting of The Institute of Navigation, Williamsburg, VA, June 1991, pp. 183-191.

Single Difference Geometry

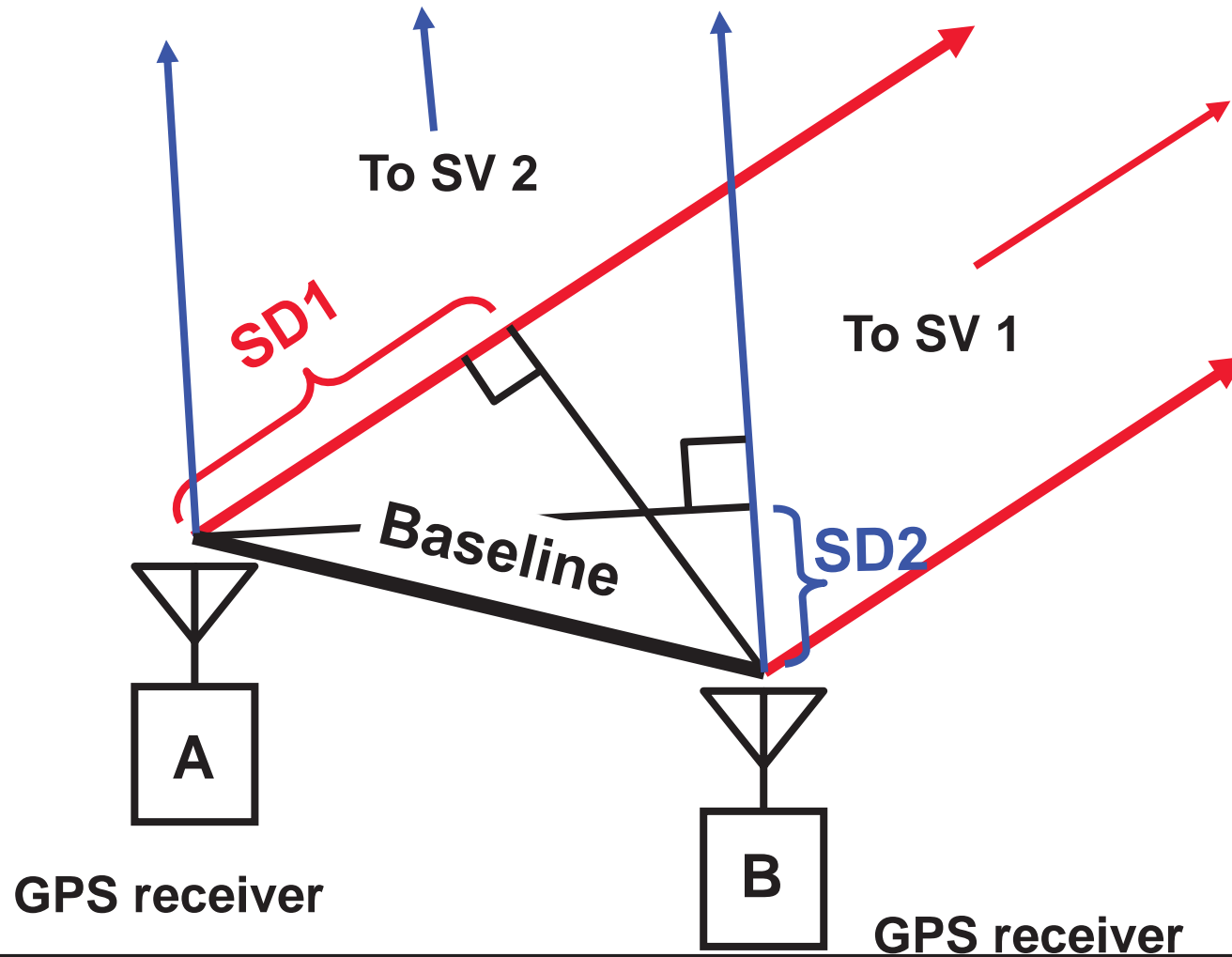


The Single Difference

- The Single Difference (SD) is taken as the difference between the measurements from two receivers for one satellite.
- The SD is the projection of the baseline vector, \underline{b} , onto the line-of-sight to the satellite
 - » Can be written as the inner-product of the baseline vector with the unit vector to the satellite.

$$SD = \underline{b} \cdot \underline{e} = \begin{pmatrix} x \\ y \\ z \end{pmatrix} (e_x, e_y, e_z) = e_x x + e_y y + e_z z$$

Double Difference Geometry



Single and Double Differences

- Two Accumulated Doppler Single Differences:

$$SD_i = \underline{b} \cdot \underline{e}_i = \phi_{i,1} - \phi_{i,2} + N_i \lambda + c \delta t_{12}$$

$$SD_j = \underline{b} \cdot \underline{e}_j = \phi_{j,1} - \phi_{j,2} + N_j \lambda + c \delta t_{12}$$

Ambiguity exists since the Doppler accumulation starts at an arbitrary value (zero, or close to the pseudorange) and the clock offset exists because the two receivers use different clocks. Cannot tell them apart !

- Double Difference:

$$DD_{ij} = SD_i - SD_j$$

$$DD_{ij} = \underline{b} \cdot (\underline{e}_i - \underline{e}_j) = \phi_{i,1} - \phi_{i,2} - (\phi_{j,1} - \phi_{j,2}) + N_{ij} \lambda$$

Double Difference Equation

- The Double Difference Equation:

$$\begin{pmatrix} DD_{1r} \\ DD_{2r} \\ DD_{3r} \end{pmatrix} = \begin{pmatrix} (\underline{e}_1 - \underline{e}_r)^T & 1 & 0 & 0 \\ (\underline{e}_2 - \underline{e}_r)^T & 0 & 1 & 0 \\ (\underline{e}_3 - \underline{e}_r)^T & 0 & 0 & 1 \end{pmatrix} \begin{pmatrix} x \\ y \\ z \\ N_{1r} \\ N_{2r} \\ N_{3r} \end{pmatrix}$$

- Four satellites are used to form 3 DDs
- One satellite is the reference
- Solve for baseline vector $(x, y, z)^T$ and three integer ambiguities: N_{1r}, N_{2r}, N_{3r}

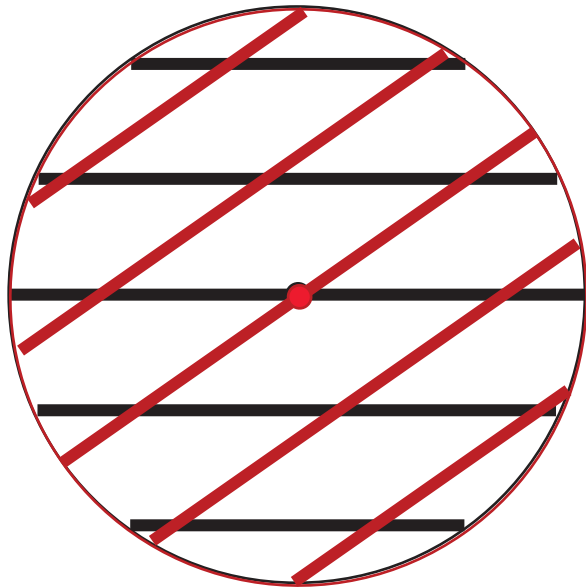
Ambiguity Resolution

- Many mathematical ambiguity search techniques, e.g.:
 - » Exhaustive search with pruning
 - » Lambda method*
- Reliability of ambiguity resolution techniques is still not at the level required for aircraft precision approach:
 - » Handling of time-varying and spatial-varying error sources (e.g. ionospheric and tropospheric propagation delays)
 - » Carrier phase robustness and cycle slip detection/repair
 - » Operation in the presence of interference
- Additional satellites (more than 6) are very helpful

* Teunissen, P.J.G., De Jonge, P.J., Tiberius, C.C.J.M, "The Lambda-Method for Fast GPS Surveying," Proceedings of the International Symposium GPS Technology and Applications, Bucharest, Romania, September 26-29, 1995.

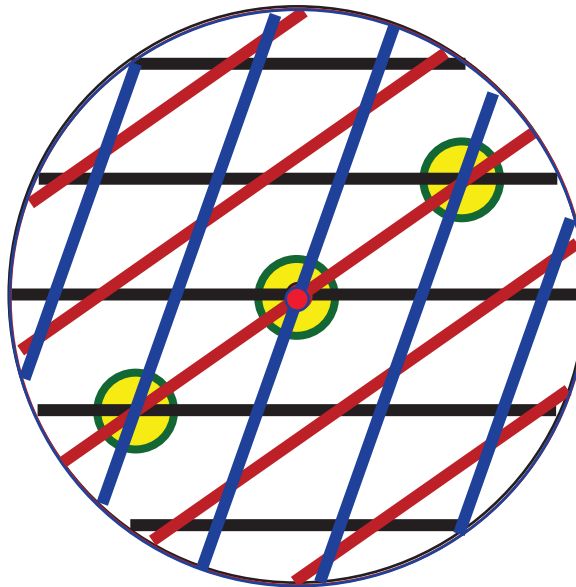
Ambiguity Resolution Concept

Two wavefronts



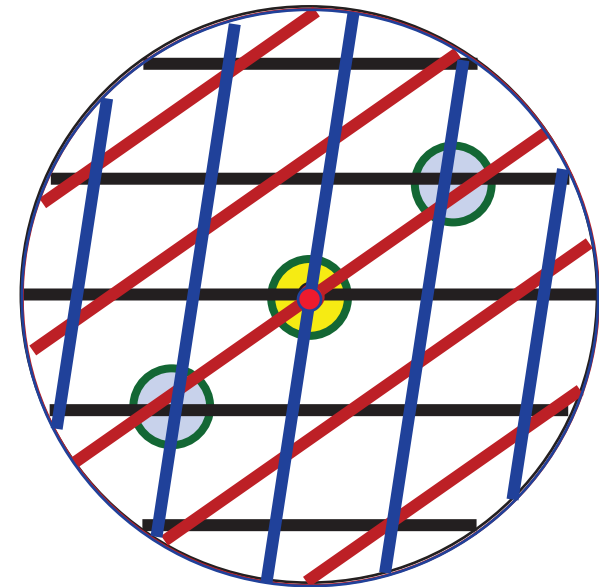
All crossings are potential position solutions

One redundant wavefront



Potential position solutions are discarded due to wavefront rotation

One redundant rotated wavefront



Helpful: additional satellites, faster geometry changes, better initial position solution, better measurements

Ambiguity Function Method

- First published method (developed in 1981)
- Select a trial position and calculate corresponding double differences
- Compare trial DDs with measured DDs using the ambiguity function (over all DDs and all epochs):

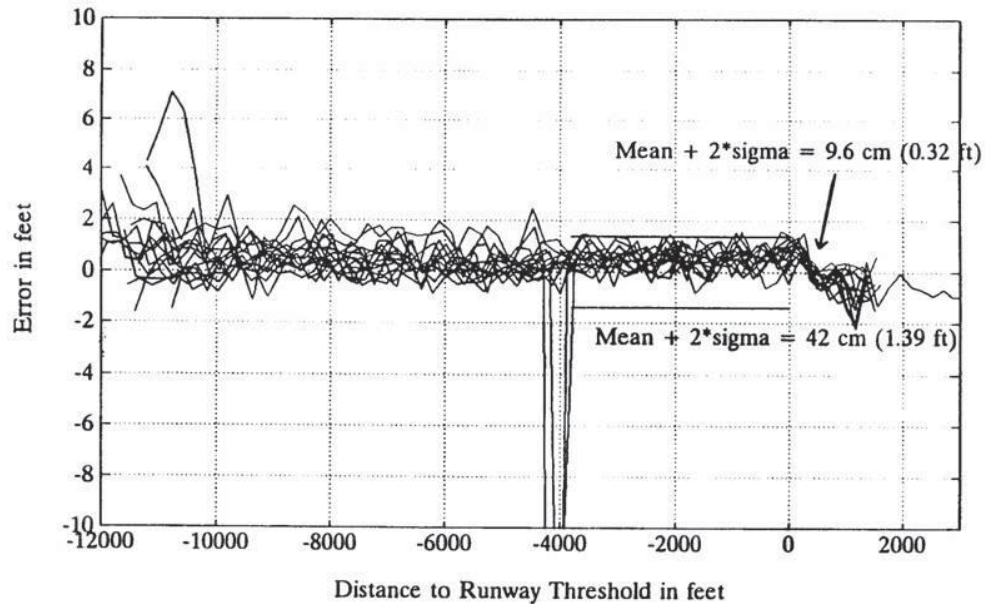
$$AF_{TRIAL} = \frac{\sum_{n=1}^N \sum_{p=1}^M \cos(DD_{MEAS}^{np} - DD_{TRIAL}^{np})}{NM}$$

- At the correct location, the ambiguity function is a maximum (insensitive to cycle slips)

Least Squares Ambiguity Search

- Developed for dynamic positioning
- Uses redundant measurements to constrain the ambiguity search
- Based on solution residuals using fault detection techniques
- Much effort was spent to reduce the computation time:
 - » If there are 5 DDs and each has an uncertainty of $\pm 5\lambda$, then a total of $(11)^5 = 161051$ potential ambiguity sets exist

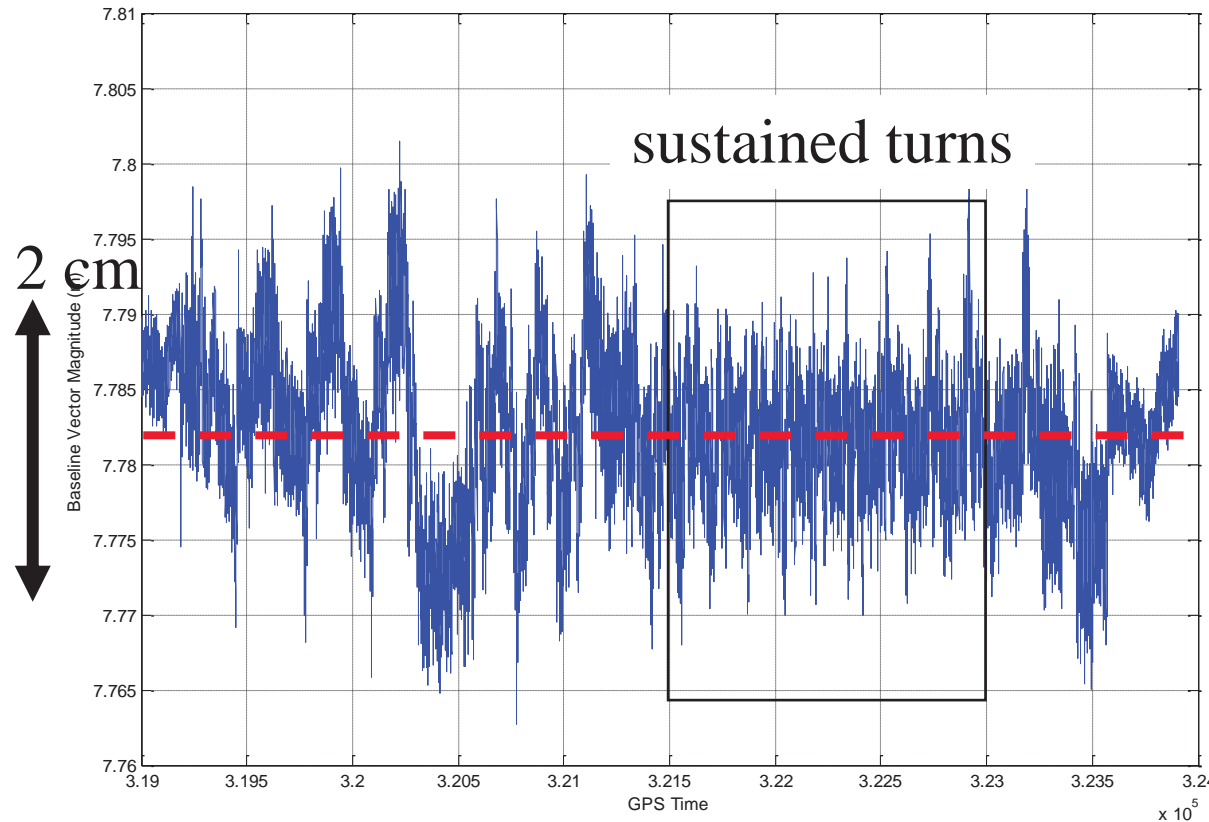
Double Difference Kinematic Performance Example



Fuselage Baseline Performance (In-Flight)

Dual-GPS Baseline Length (7.8 m)

DC-3 multipath can be several centimeters



During sustained turns: multipath “oscillates” and becomes zero-mean

baseline



Length: rms ≈ 0.7 cm
→ Lateral rms ≈ 0.7 cm
0.7 cm over 7.8 m
→ 0.9 mrad noise

Triple Difference

- Use Double Differences at two time intervals; this cancels the ambiguities:

$$\text{Time 1: } \underline{DD}_1 = H_1 \underline{b}_1$$

$$\text{Time 2: } \underline{DD}_2 = H_2 \underline{b}_2$$

- Triple Difference:

$$\underline{TD} = \underline{DD}_2 - \underline{DD}_1 = H_2 \underline{b}_2 - H_1 \underline{b}_1$$

$$\underline{TD} = H_2 (\underline{b}_1 + \underline{\Delta b}) - H_1 \underline{b}_1$$

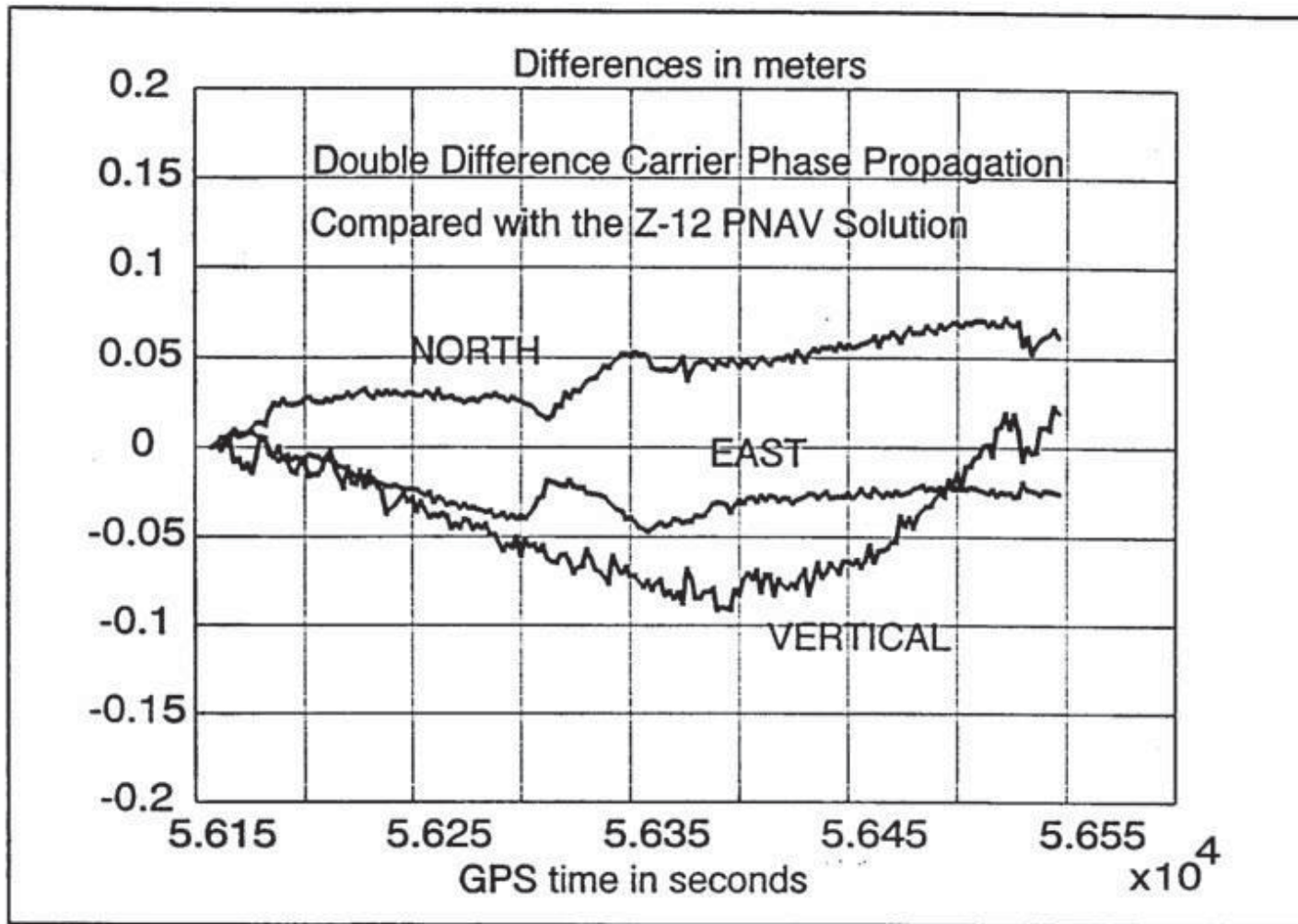
- Change in position:

$$\underline{\Delta b} = \left(H_2^T H_2 \right)^{-1} H_2^T \left(\underline{TD} - (H_2 - H_1) \underline{b}_1 \right)$$

Triple Difference Propagation

- Triple Differences (from accumulated carrier phase) can be used to accurately propagate the receiver's position with centimeter-level accuracy
- The term: $(H_2 - H_1)\underline{b}_1$ corrects for the change in geometry from time 1 to time 2
 - » Without this term, a small error, on the order of one centimeter, would be introduced
 - » This error would be systematic and would therefore accumulate over time; e.g. after 100 seconds, the error would grow to 1 meter
- By using the TD propagation, a dynamic user becomes essentially static from a processing point of view (will only vary position within centimeters)

Triple Difference Flight Test Data

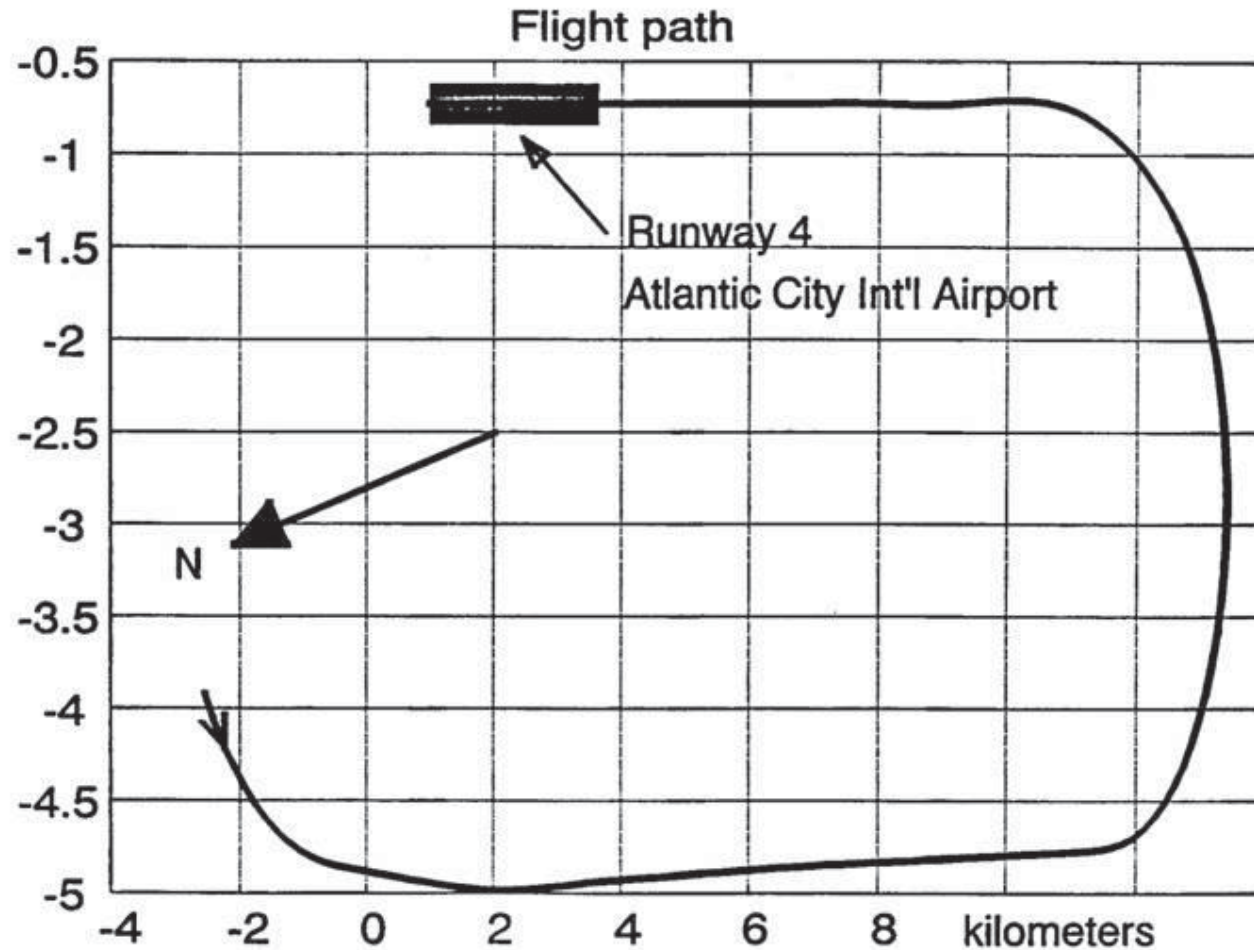


Integrated Doppler DD Method

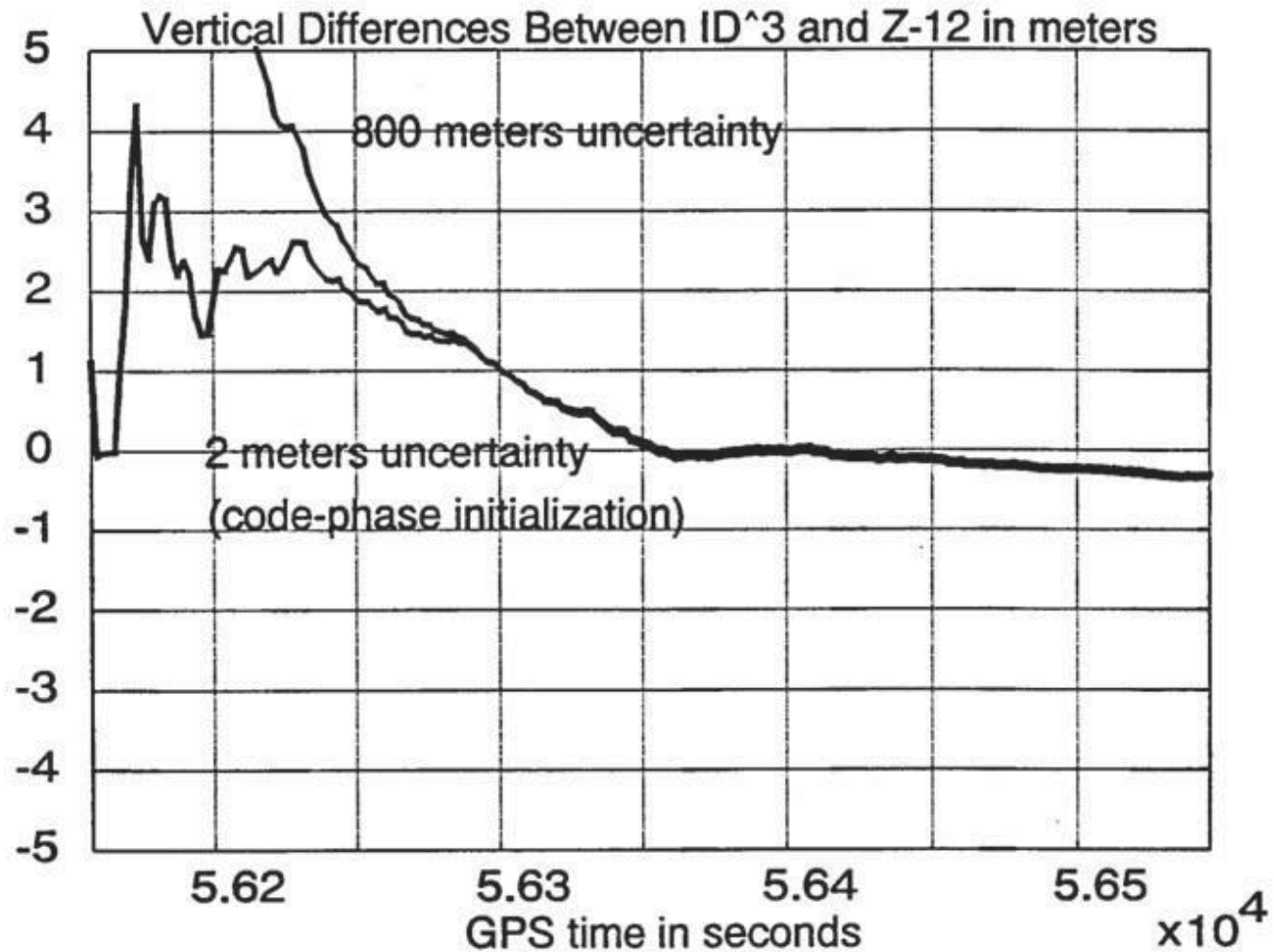
- Uses both redundant measurements and changing geometry to estimate the aircraft position in a Kalman filter with Triple Difference propagation
- Method also works in the absence of code phase measurements: Doppler positioning
- Convergence time is typically 2 minutes using 7 satellites
- Feasibility of this method was shown in a flight test with a Boeing 757 at Atlantic City Int'l Airport

Ref: Van Graas, F. and Shane-Woei Lee, "High-Accuracy Differential Positioning for Satellite-Based Systems without Using Code-Phase Measurements," NAVIGATION: Journal of The ION, Vol. 42, No. 4, Winter 1995-1996.

Aircraft Flight Path



Vertical IDM Performance



Other Techniques

- Use multiple frequencies to obtain the so-called widelane (e.g. L1-L2 = 347.82 MHz, $\lambda = 86.19$ cm)
 - » Reduces the number of ambiguity sets
 - » Same can be done with L5
- Use ground-based pseudolites to provide for a fast geometry change
- Add satellites from other constellations: Glonass, Compass, Galileo
- Avoid ambiguity resolution, but perform extensive carrier phase smoothing instead

Overview

- High precision GPS techniques
 - » Relative, differential, wide area differential
 - » Kinematic, surveying, attitude determination
- GPS code and carrier phase measurements
 - » Error sources: Clock and orbit errors, ionospheric and tropospheric propagation delays, multipath, noise, antenna phase and group delays
- Additional implementation considerations

GPS Differential Error Sources

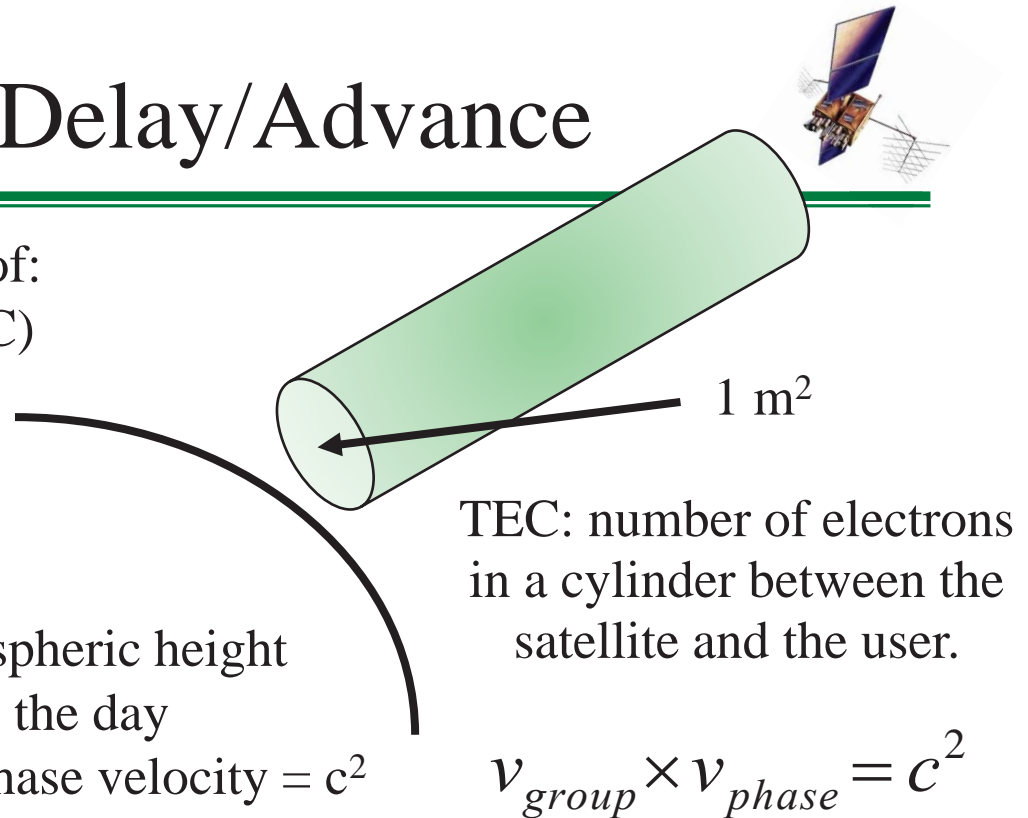
Range Error Sources		Relative/Differential System	
Baseline		Up to 50 km	Up to 200 km
Normal operation condition (carrier phase)	Ionosphere (dual freq)	< 0.5 cm	< 3 cm
	Troposphere	< 1 cm	1-2 cm
	SV orbit error	< 1 cm	10 cm
	SV clock error	N/A	N/A
	Multipath	< 0.5 cm	< 0.5 cm
	Receiver noise	< 0.5 cm	< 0.5 cm
	Receiver antenna	< 0.2 cm	< 0.2 cm
	Composite (RSS largest)	1.7 cm	10.7 cm
Performance limitations	Ionosphere storm	1-3 cm	1-3 cm
	Troposphere storm	1-30 cm	1-30 cm
	SV anomalies	1 cm	30 cm
	Composite (RSS largest)	30 cm	44 cm

Errors Affecting Differential Applications

- Ionosphere, troposphere, satellite orbit, multipath, noise, antenna phase and group delays
- Other errors that need to be corrected:
 - » Carrier phase wrap-up
 - Stationary, dynamic
 - » Receiver dynamics-related errors
 - » Earth tides, ocean loading, plate tectonics, satellite antenna
- Errors that don't need to be corrected (are common and cancel between two receivers):
 - » Satellite clock
 - » Satellite inter-frequency and inter-code biases

Ionosphere Delay/Advance

- Ionospheric delay is a function of:
 - » Total Electron Content (TEC)
 - Solar cycle
 - Diurnal effect
 - Geomagnetic latitude
 - » Frequency
 - » Elevation angle: Mean ionospheric height
- Few ns at night to 100 ns during the day
- Product of group velocity and phase velocity = c^2
- Phase Advance = - Group Delay
- Pseudorange travels at the group velocity and is delayed through the Ionosphere
- Carrier phase travels at the phase velocity and is advanced through the ionosphere.
- This phenomenon is referred to as Code-Carrier Divergence, which is on the order of 3 ns (or 1 m) per 10 minutes (elevation angle dependent).



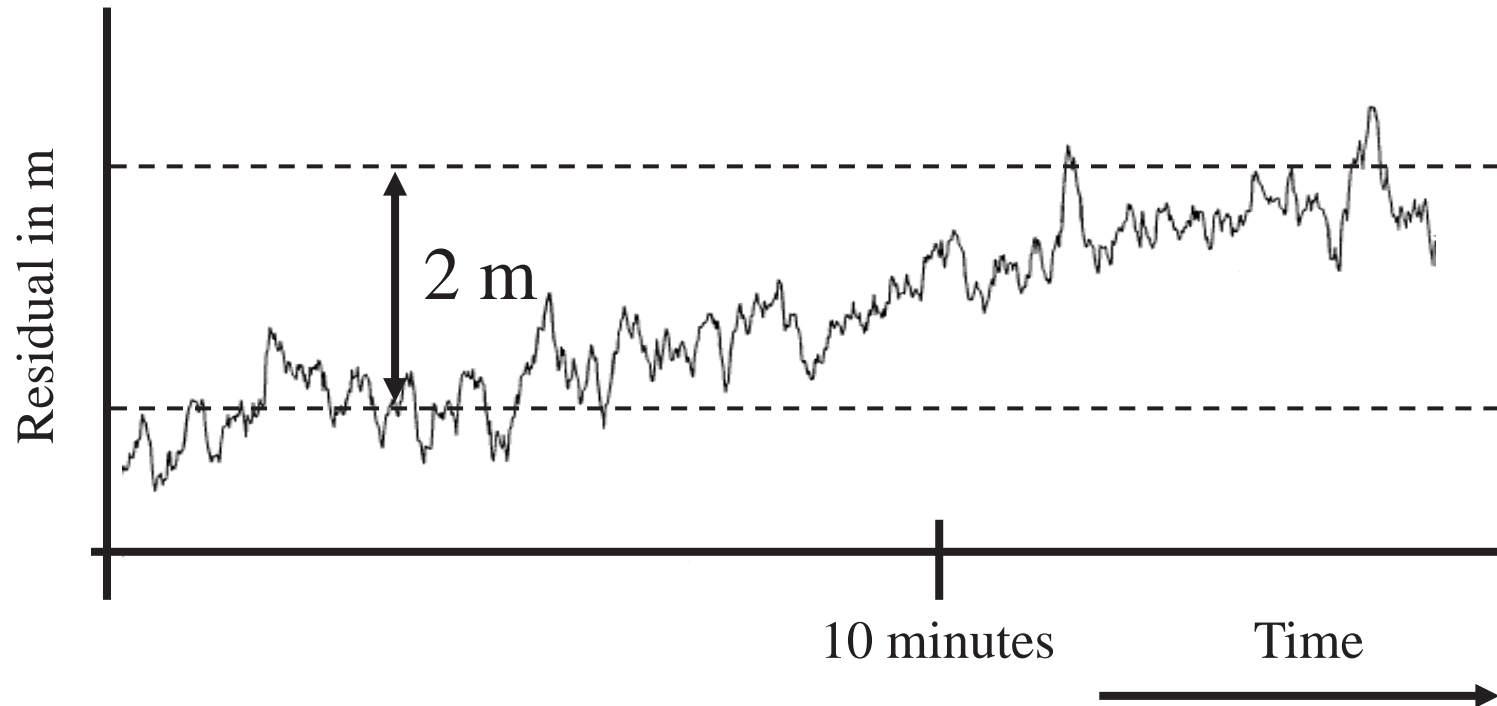
Code-Carrier Divergence

- Code-minus-carrier analysis is often used for evaluating GPS pseudorange performance, or monitoring changes in the ionospheric delay:

$$\text{CMC}(t) = \rho(t) - \int_0^t \phi(t) dt$$

- Most errors are common between the pseudorange and the integrated carrier phase, except for
 - » Multipath (much smaller on the carrier)
 - » Thermal noise (much smaller on the carrier)
 - » Ionospheric delay

Code-Carrier Divergence Example



Code-carrier divergence can be removed using dual-frequency measurements.

Ionosphere Errors

$$1 \text{ TECU} = 10^{16} \text{ el/m}^2$$

Approx. delay:

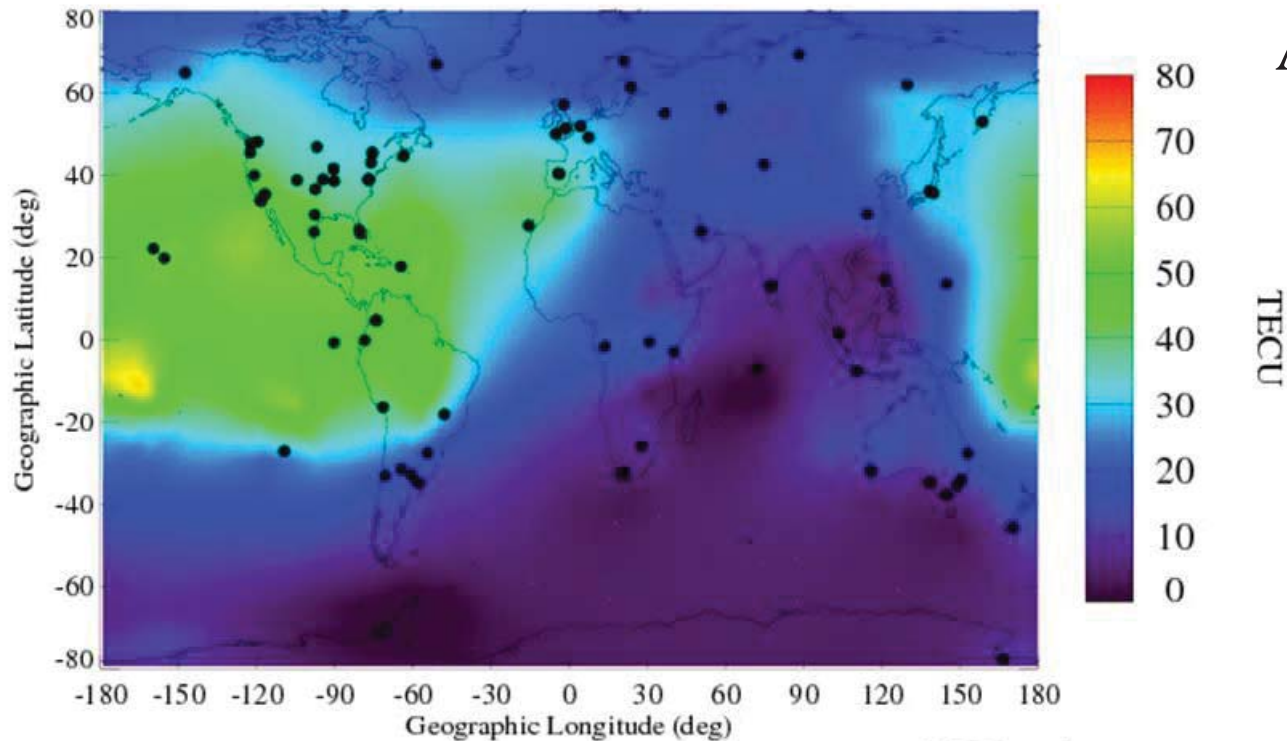
$$I_i = \frac{40.3 \text{TEC}_i}{f_i^2}$$

$$1 \text{ TECU}_1 \approx 16 \text{ cm} \\ (\text{at GPS } L_1)$$

$$1 \text{ TECU}_2 \approx 27 \text{ cm} \\ (\text{at GPS } L_2)$$

06/02/12
21:00 UT

Ionospheric TEC Map

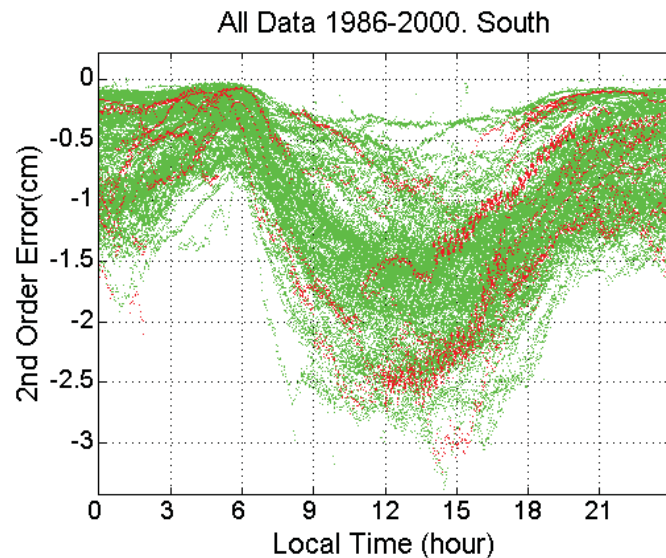


• GPS Receiver

From: http://iono.jpl.nasa.gov/latest_rti_global.html

Higher-Order Ionospheric Effects

- Example second-order error at Arecibo



Arecibo Incoherent Scattering Radar
Over 14 years of radar data
>2660 hours measurements

(amounts to approximately half of
the GPS error – up to 600 km)

$$\rho_i = r + \frac{q}{f_i^2} + \frac{s}{f_i^3} + \frac{r}{f_i^4} + \dots + M_{\rho,i} + \delta r + \varepsilon_{\rho,i}$$

Research performed with Miami Univ (Dr. Jade Morton)
supported by AFOSR (Dr. Jon Sjogren)

Differential Ionosphere Errors

- For single frequency users
 - Rely on correlated ionosphere errors over small baselines between receivers (< 5 km)
 - Remaining error is small (less than 1 cm) when the ionosphere is quiet, but errors can grow quickly during ionospheric gradients
- For dual frequency users
 - Measure both frequencies
 - Increases noise
 - Corrects approximately 99% of the delay
 - Valid for larger baselines (limited by decorrelation of higher-order ionospheric corrections – few cm)

Dual Frequency Ionosphere Correction

ionosphere-free
pseudorange

$$\rho_{L1,corr}(t) = \rho_{L1}(t) - I_{L1}(t) =$$

$$\rho_{L1}(t) - (\rho_{L1}(t) - \rho_{L2}(t)) \frac{f_{L2}^2}{f_{L2}^2 - f_{L1}^2}$$

ionosphere-free
carrier phase

$$\phi_{L1,corr}(t) = \phi_{L1}(t) + I_{L1}(t) =$$

$$\phi_{L1}(t) - (\phi_{L2}(t) - \phi_{L1}(t)) \frac{f_{L2}^2}{f_{L2}^2 - f_{L1}^2}$$

- L_1 and L_2 carrier phase can be used to calculate changes in $I_{L1}(t)$, which, in turn can be used to smooth the L_1 pseudorange

Troposphere Delays

- Affects L1, L2, code and carrier equally
- Delay is a function of temperature, humidity, pressure, and path through the troposphere
 - » Dry delay (hydrostatic) 2-2.5 m in the zenith direction, highly predictable
 - » Wet delay (water vapor) up to 0.4 m in the zenith direction, difficult to model

- Zenith Delay:

$$ZD(m) = \int_0^h 10^6 (n - 1) dz$$

n is index of refraction

Zenith delays at sea level

Dry air: 250 cm

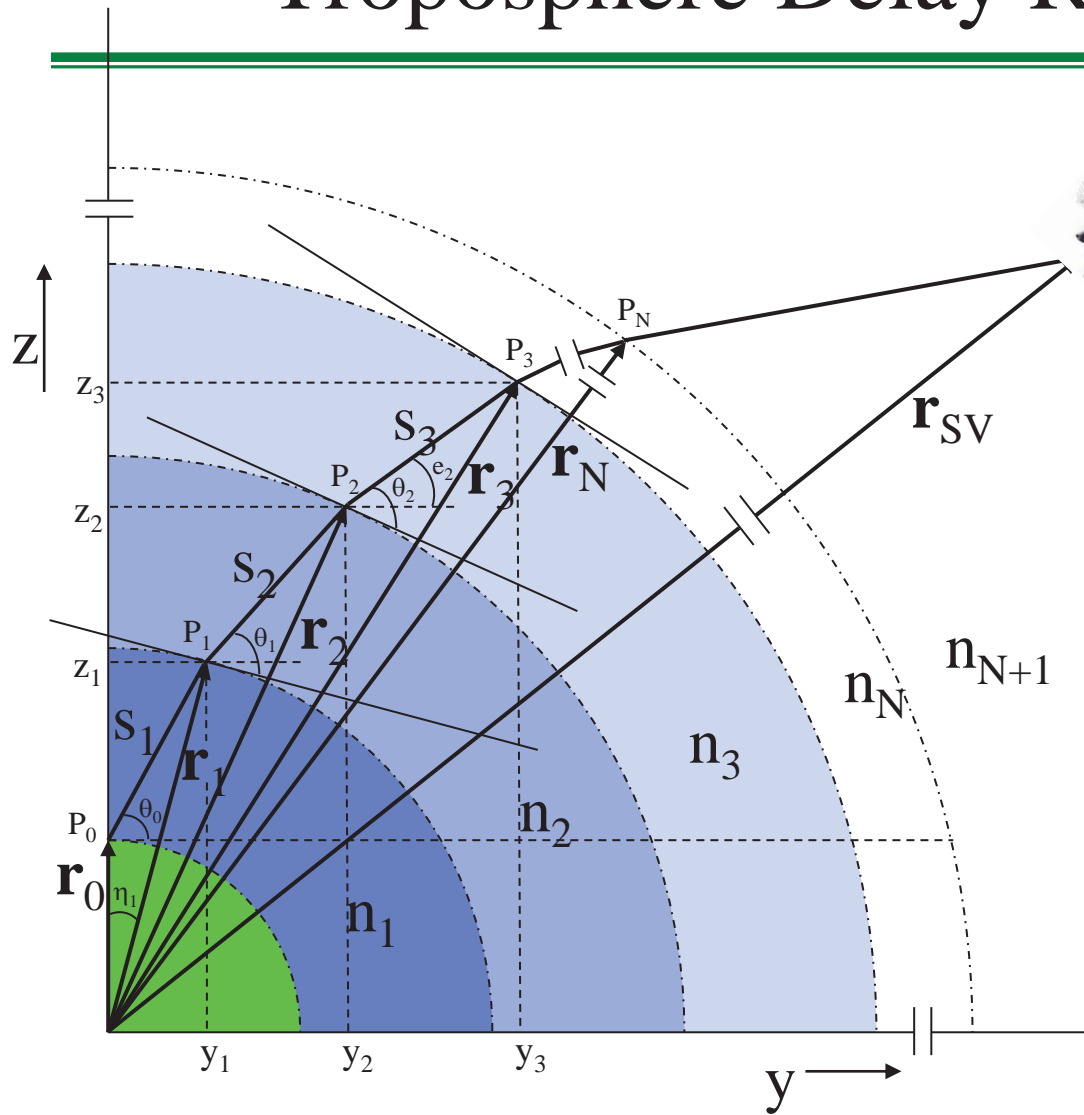
Water vapor: 40 cm

Hydrometeors: 1.5 cm

Differential Troposphere Errors

- For single frequency users
 - Rely on correlated troposphere errors over small baselines between receivers (< 5 km)
 - Remaining error is small (less than 1 cm) when the troposphere is quiet, but errors can grow quickly during weather events
 - Only correction for weather events is a detailed tropospheric model \rightarrow need knowledge of the conditions along the entire path through the troposphere
- For dual frequency users
 - Same as for single frequency – no dual-frequency correction possible

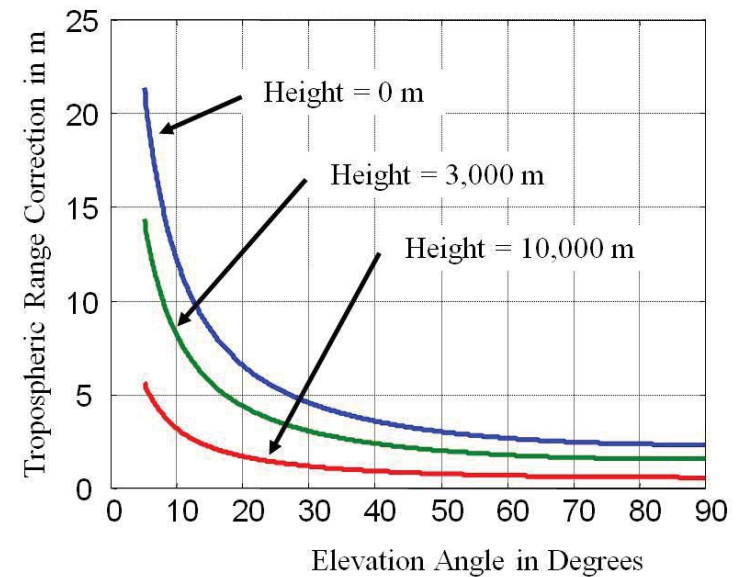
Troposphere Delay Ray Tracing



Delay and refraction

$$d_{tropo} = d_{s,h} + d_{s,w} + d_{geo}$$

$$d_{geo} = |\mathbf{r}_{SV} - \mathbf{r}_0| + |\mathbf{r}_{SV} - \mathbf{r}_N| + \sum_{i=1}^N s_i$$

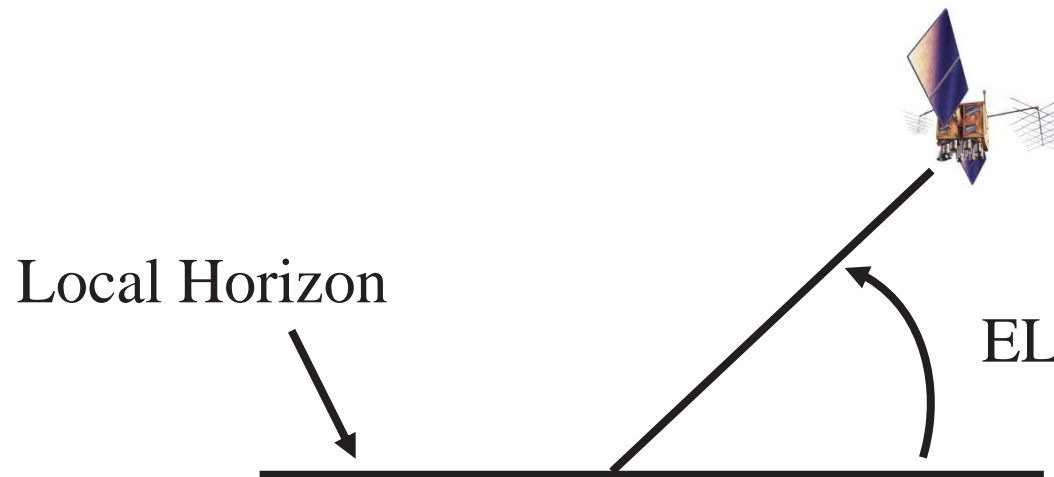


Simple Troposphere Model

- Removes approximately 90% of the tropospheric delay error:

$$\text{delay} = \frac{2.4224e^{-0.13345 \times 10^{-3} H}}{0.026 + \sin(EL)} \quad (\text{m})$$

where: EL is the elevation angle; H is the height (m)



Modified Hopfield Model

- Removes approx. 98% of the nominal troposphere delay:

$$\text{delay} = 10^{-6} N_1 \sum_{j=1}^9 A_{j1} \frac{R_1^j}{j} + 10^{-6} N_2 \sum_{j=1}^9 A_{j2} \frac{R_2^j}{j}$$

$$N_1 = 77.624 \frac{p}{T} \quad N_2 = -12.92 \frac{e}{T} + 3.719 \times 10^5 \frac{e}{T^2}$$

$$R_i = \sqrt{(a_e + h_i)^2 - a_e^2 \cos^2(EL)} - a_e \sin(EL), \quad i=1,2$$

$$h_1 = 5 \frac{0.002277p}{N_1 10^{-6}} \quad h_2 = 5 \frac{0.002277}{N_2 10^{-6}} \left(\frac{1255}{T} + 0.5 \right) e$$

$$A_{1i} = 1 \quad A_{2i} = 4a_i \quad A_{3i} = 6a_i^2 + 4b_i \quad A_{4i} = 4a_i(a_i^2 + 3b_i)$$

$$A_{5i} = a_i^4 + 12a_i^2 b_i + 6b_i^2 \quad A_{6i} = 4a_i b_i (a_i^2 + 3b_i)$$

$$A_{7i} = b_i^2 (6a_i^2 + 4b_i) \quad A_{8i} = 4a_i b_i^3 \quad A_{9i} = b_i^4$$

$$a_i = -\sin(EL) / h_i \quad b_i = -\cos^2(EL) / (2a_e h_i)$$

$$e = 6.108 \text{RH} \exp\left(\frac{17.15T - 4684}{T - 38.45}\right)$$

$i = 1$: dry component

$i = 2$: wet component

T = surface temperature in (K)

p = atmospheric pressure (mbar)

e = water vapor partial pressure (mbar)

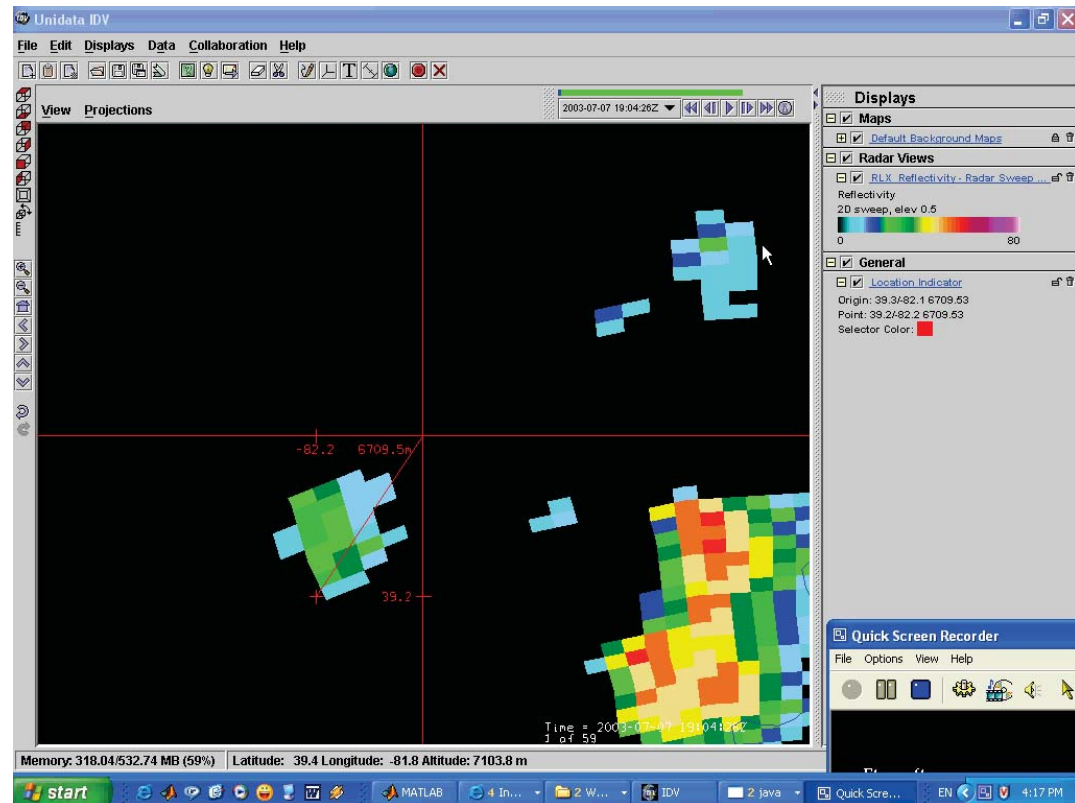
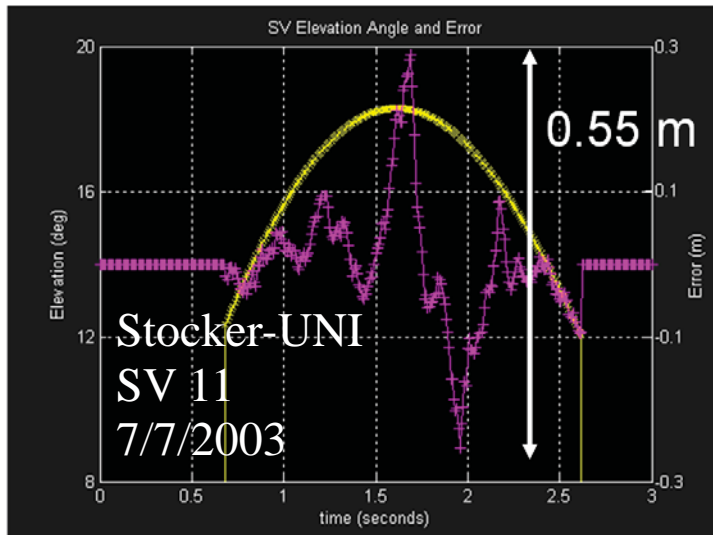
EL = elevation angle

a_e = semi-major axis of earth ellipsoid

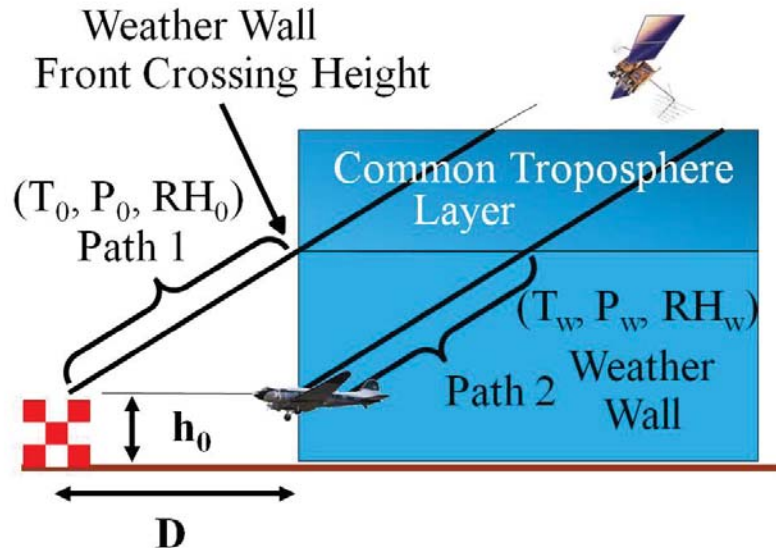
RH = relative humidity (percentage)

Troposphere Anomalies Affecting DGPS

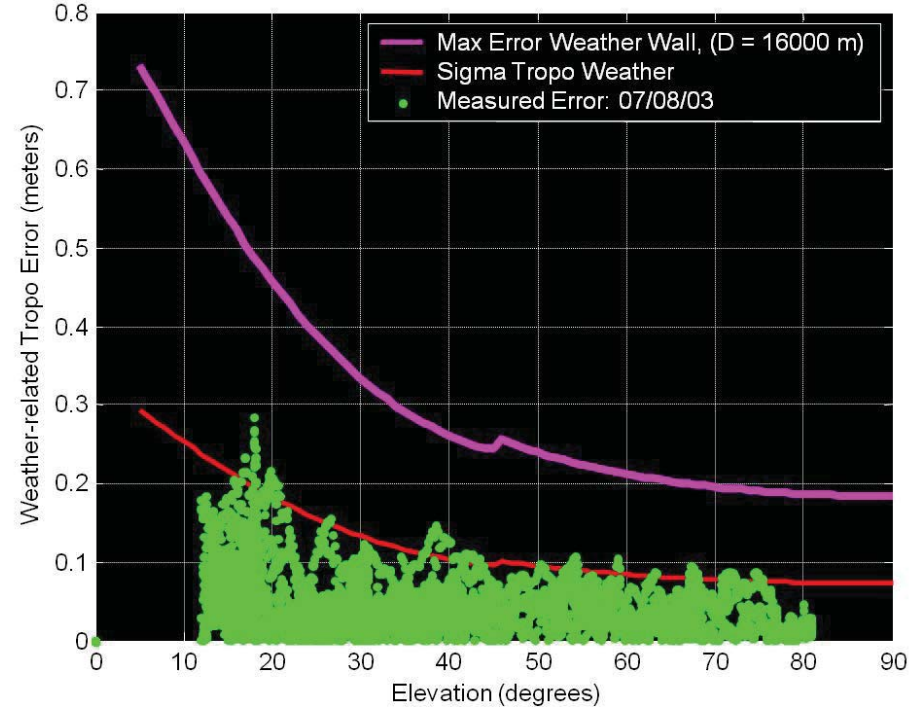
- Data collection experiments revealed unexpected decorrelation errors: 0.55 m over 16.67 km



Weather Differentials



(T, RH, P) = (26 +/- 5 Deg C, 75 +/- 25 %, 1013.25 mbars)

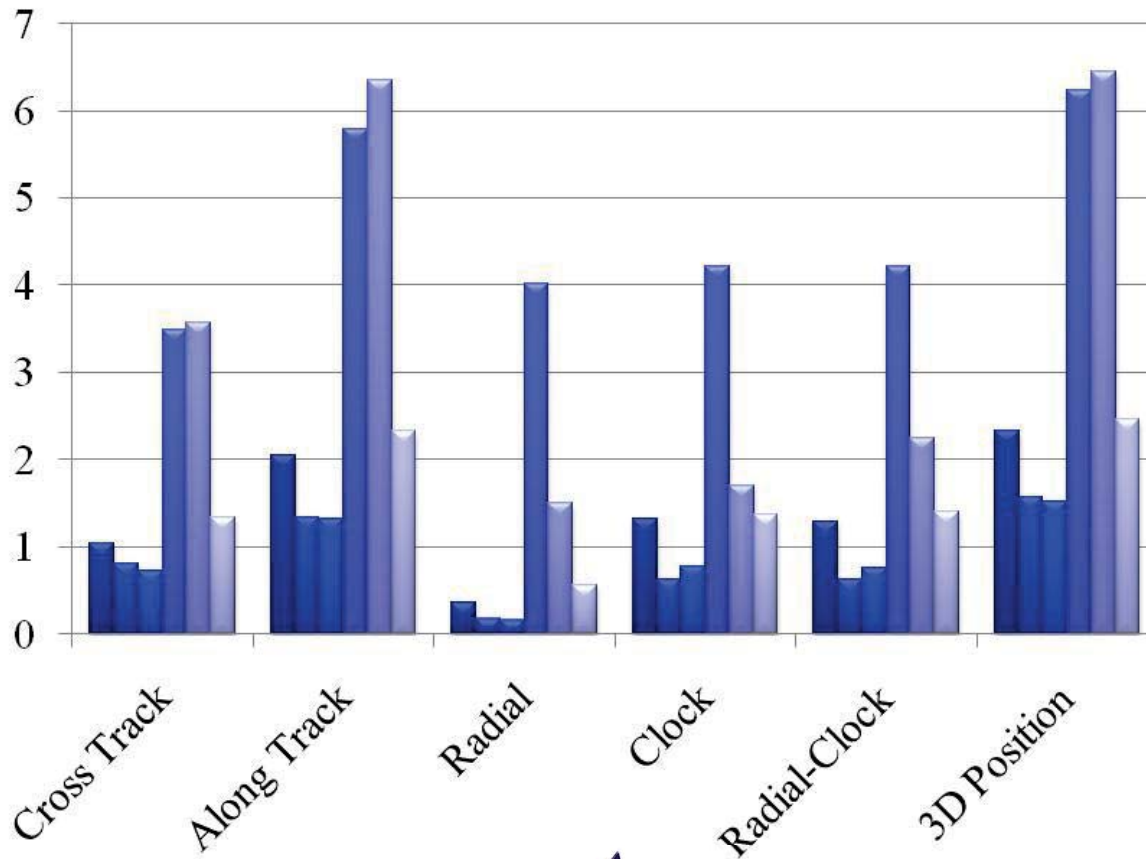


Parameter	Nominal Value	Span
Temperature °C	25 °C	± 5 °C
Relative Humidity RH	60%	± 40%
Pressure	1013.25 mbar	0

Tropospheric differentials due to severe weather can be as large as ± 0.3 m over a 5-km distance

Zhu, Z., Van Graas, F., Tropospheric Delay Threats for the Ground Based Augmentation System, ION ITM 2011.

GPS Clock and Orbit Error Statistics (m)



June 2005-June 2008

- IIA-sigma
- IIR-sigma
- IIR-M-sigma
- IIA-sigmaOB
- IIR-sigmaOB
- IIR-M-sigmaOB

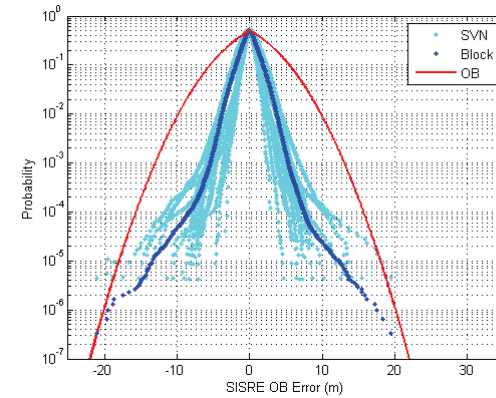


IIA



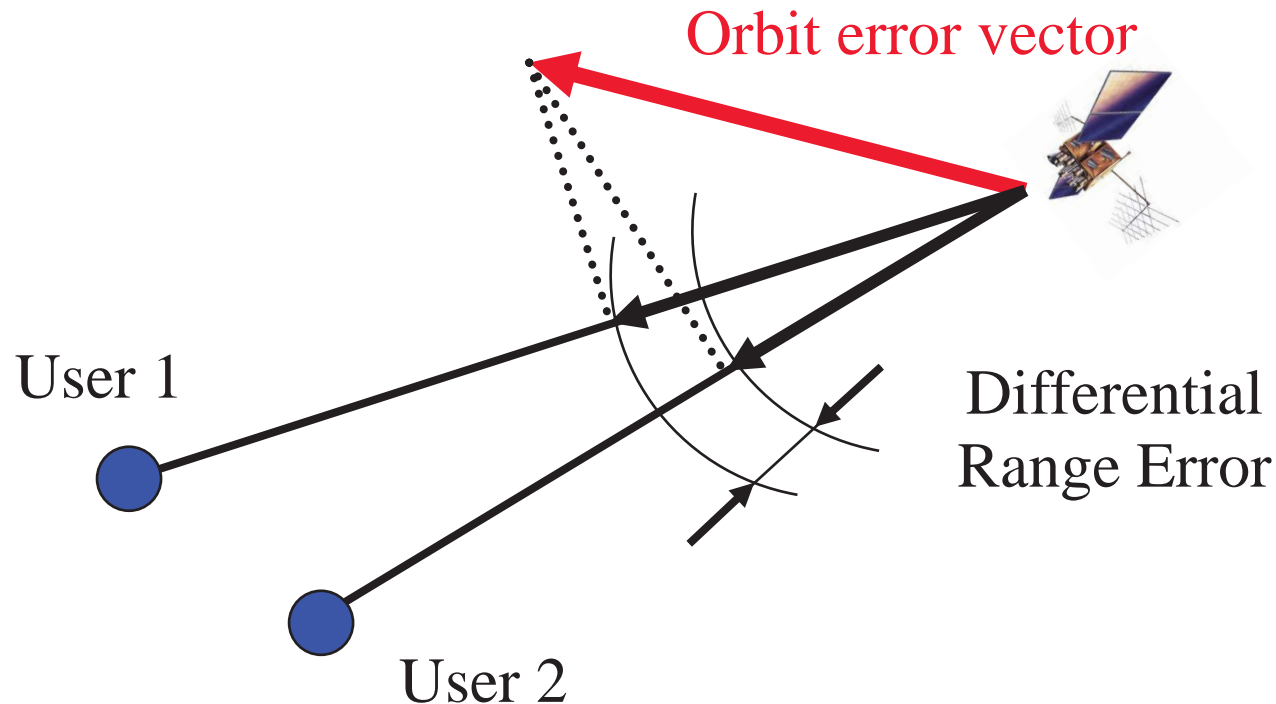
IIR

IIR-M



Spatial Decorrelation – Satellite Error

- Clock Error: Is the same in all directions and is therefore common between two receivers
- Orbit Error: Separated users observe different orbit errors



Satellite Orbit Errors

- Typical Satellite Orbit Errors
 - » Radial (RAD) 0.3 m
 - » Alongtrack (ATK) 1.5 m
 - » Crosstrack (XTK) 1.0 m

$$\text{Differential Range Error} \approx \frac{b d}{R}$$

b is the separation distance

d is the satellite position error (ATK or XTK)

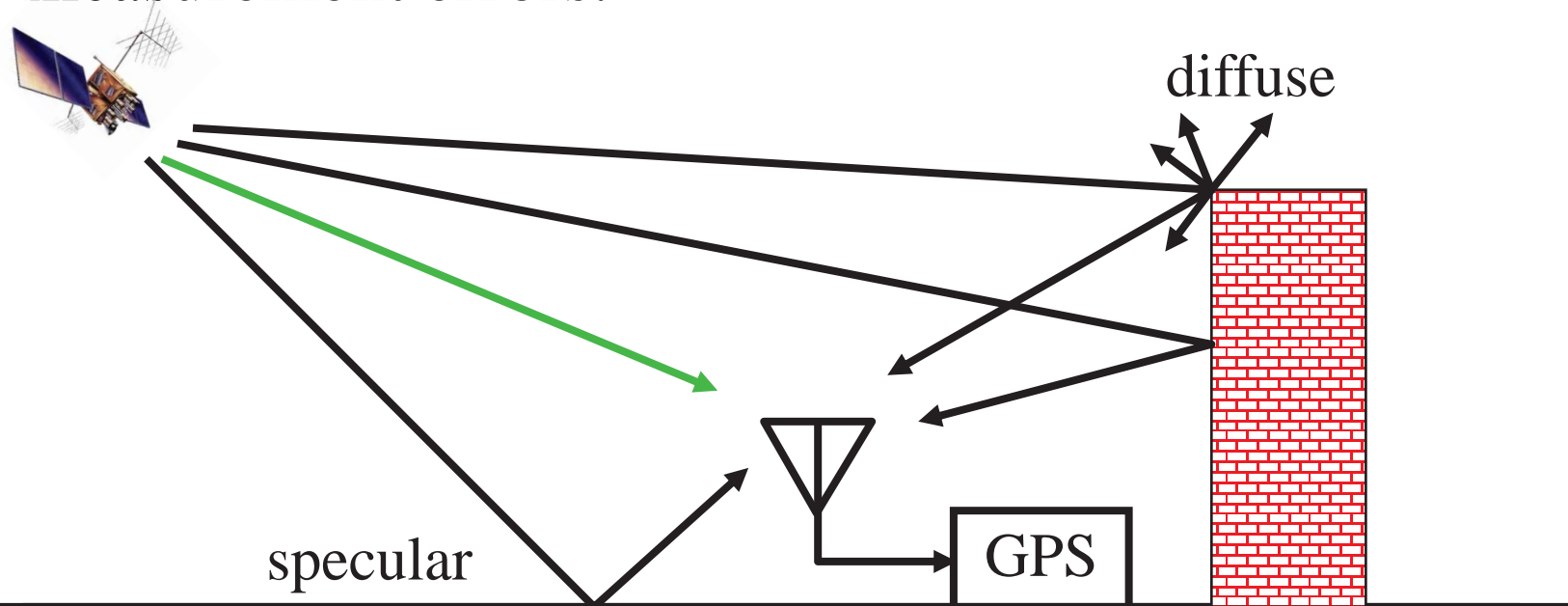
R is the satellite altitude ($\approx 11,000$ nmi)

Differential Orbit Error Examples

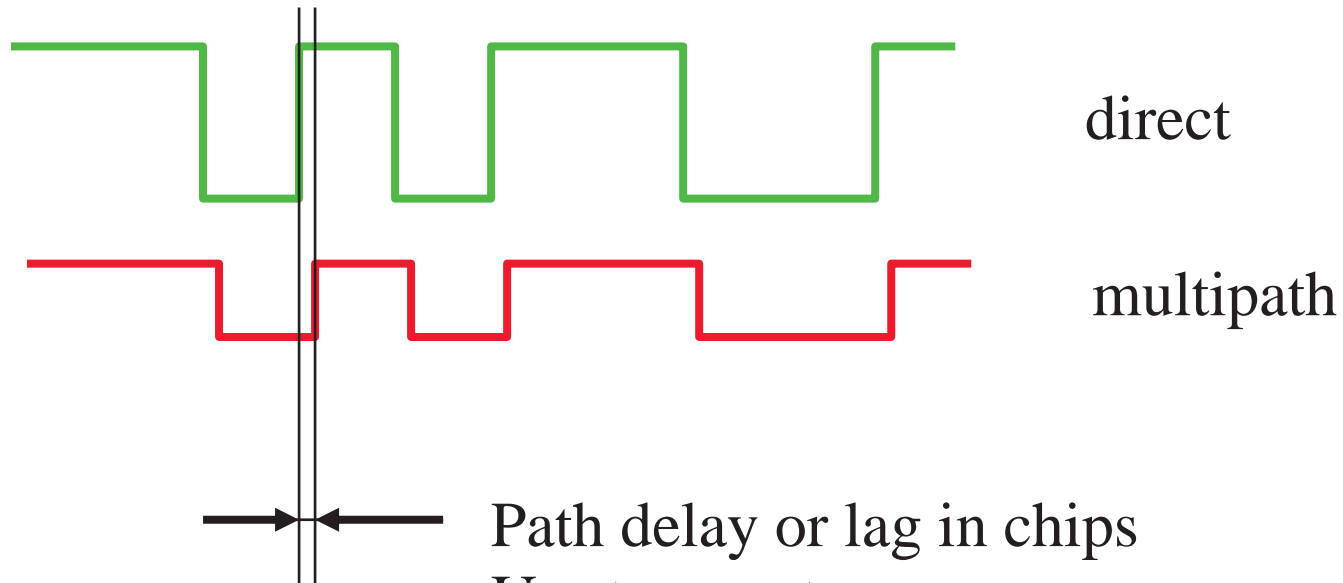
- If ATK or XTK is 5 m, and the separation distance is 100 km, then:
 - » Differential range error = $0.005 \times 5 = 2.5$ cm
- Same ATK, but separation distance is 1000 nmi:
 - » Differential range error = $0.09 \times 5 = 0.45$ m
- Differential range error:
 - » Approximately 10% of ATK or XTK per 1000 nmi separation
 - » Less than 3% of RAD (at maximum separation distance of ≈ 2000 nmi)
- Solution: (near) real-time orbit corrections (e.g. IGS)

Multipath

- The phenomenon whereby a signal arrives at the receiving antenna via multiple paths due to reflection and diffraction.
- Effect: Distortion of code and carrier phase, causing measurement errors.



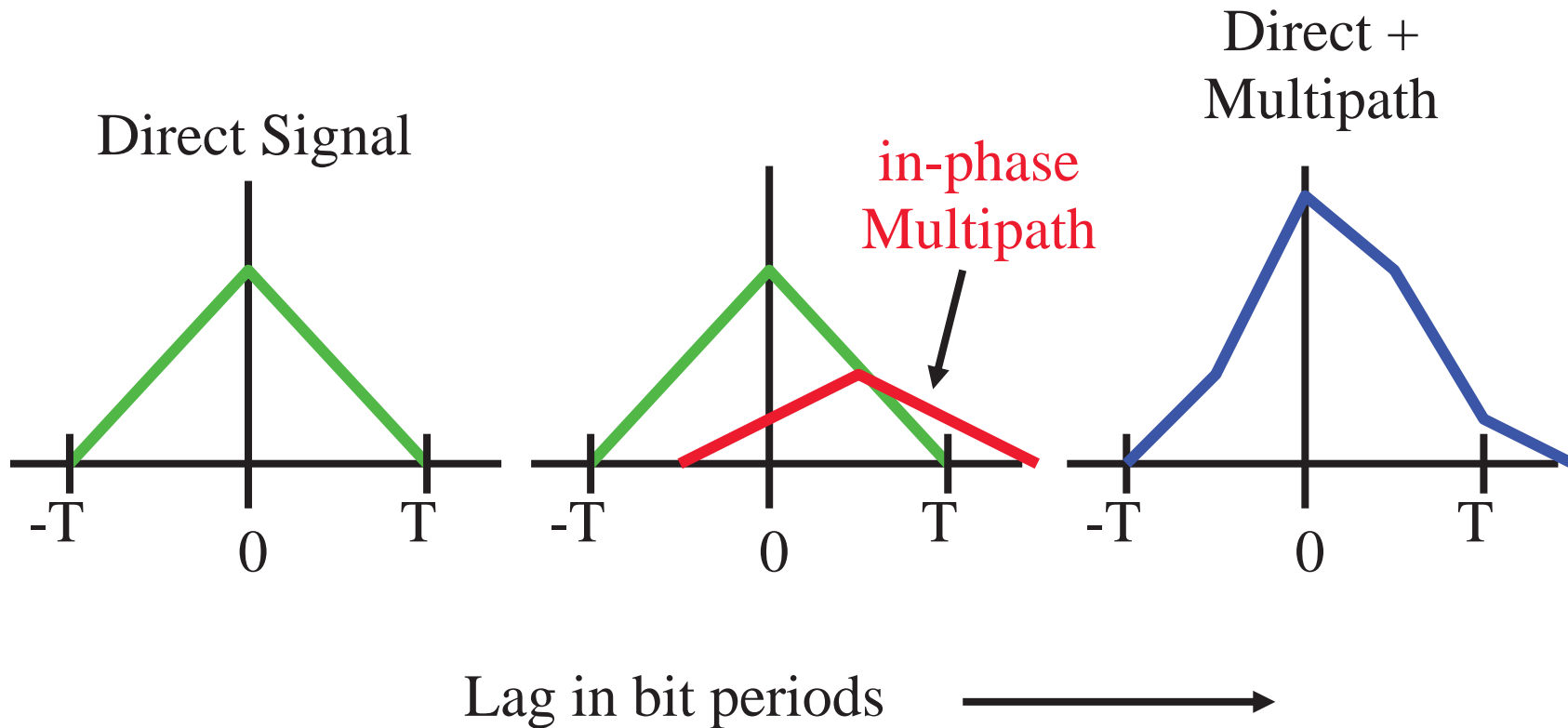
C/A Code Multipath



Use two parts:

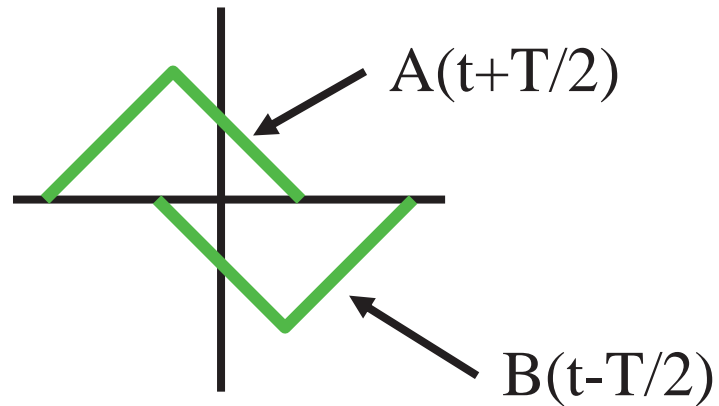
- Path delay
- Phase delay for carrier

Correlator Function

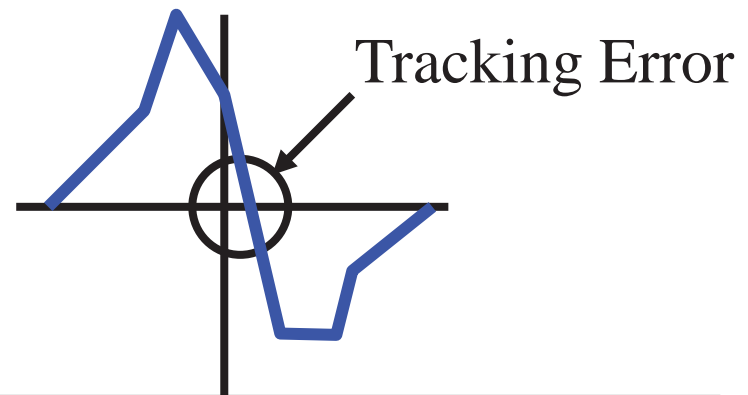
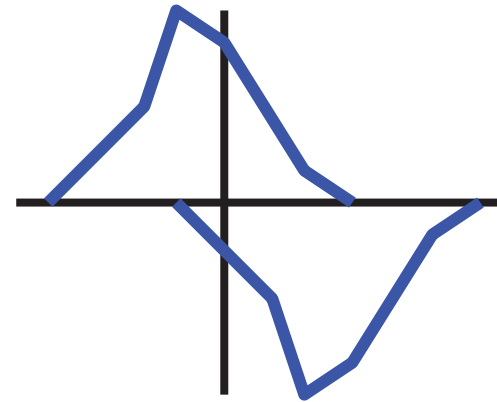


Discriminator Function

No Multipath



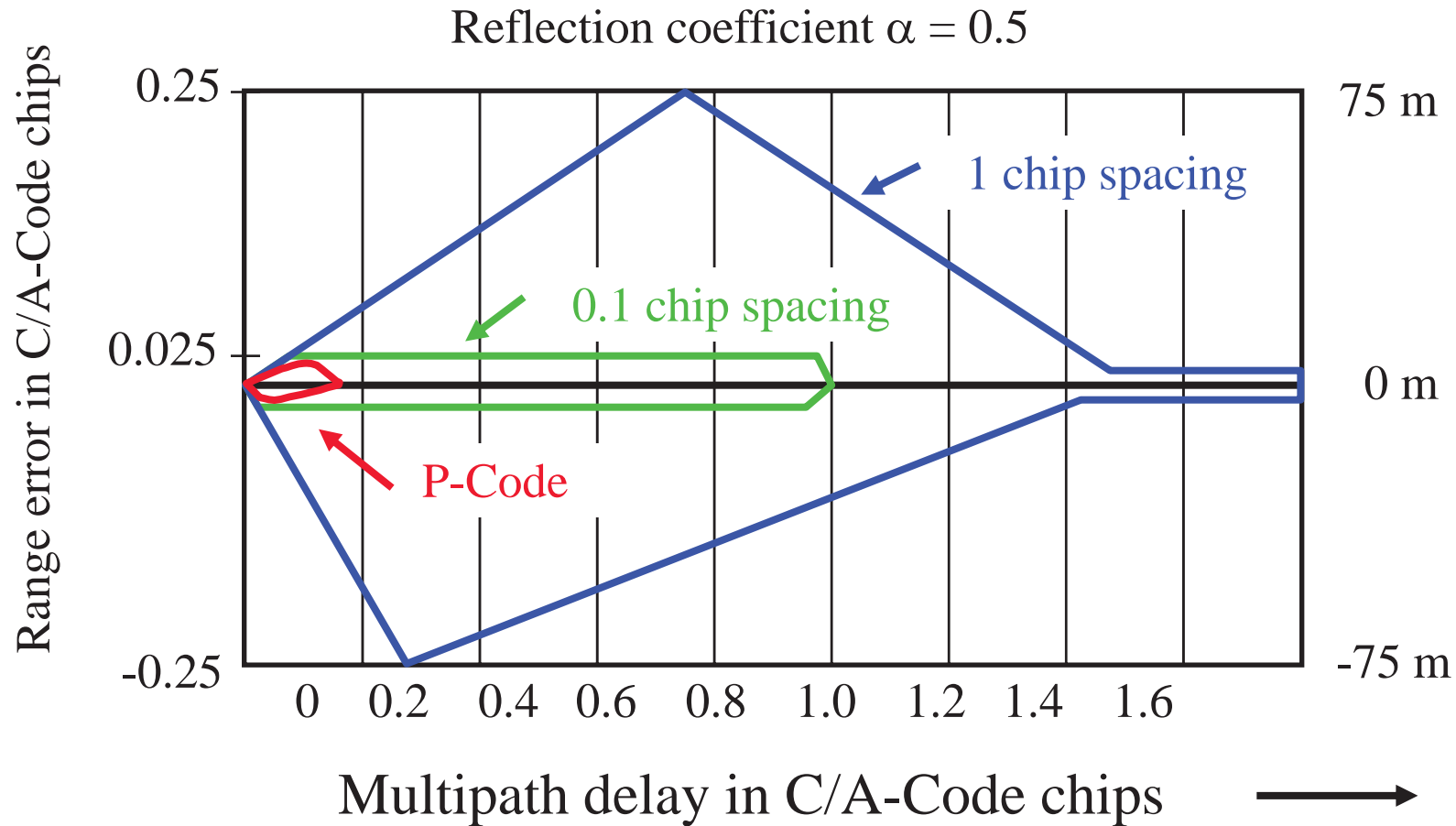
With In-Phase Multipath



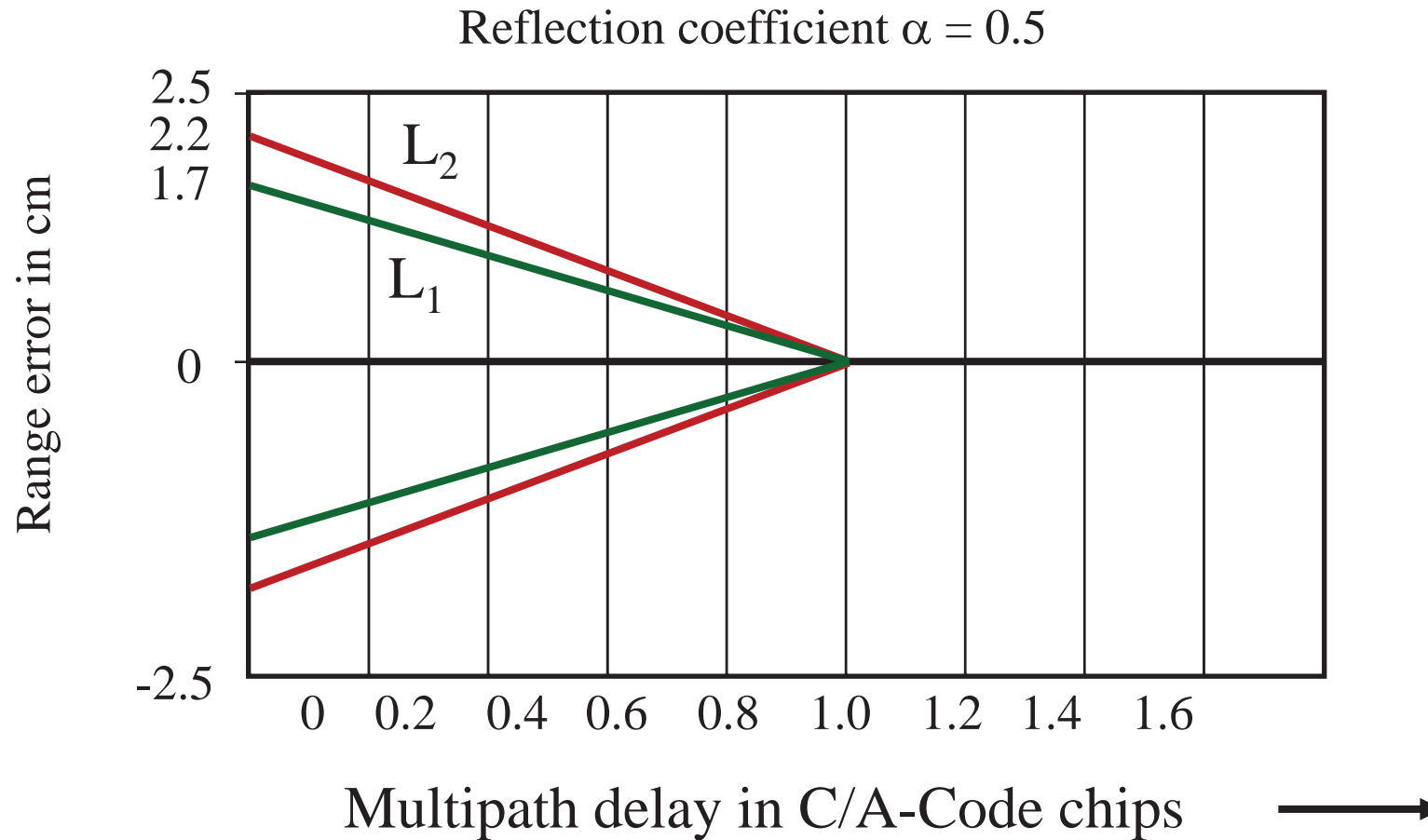
Multipath Error

- Assume that the direct signal is the strongest signal.
- Maximum code error is $\alpha\delta T/2$, where T is the bit period (≈ 293 m), α is the relative multipath strength, and δ is the correlator spacing. For $\alpha = 1$:
 - » C/A-Code (1-chip spacing): 150 m
 - » C/A-Code (0.1-chip spacing): 15 m
 - » P-Code (1-chip spacing): 15 m
- C/A-Code error is attenuated by approx. 20 dB for delays longer than $1.5T$ ($1.0T$ for 0.1-chip spacing)
- Maximum phase error is 90 degrees, or approximately 4.8 cm at GPS L1.

GPS Code Multipath Error Envelopes

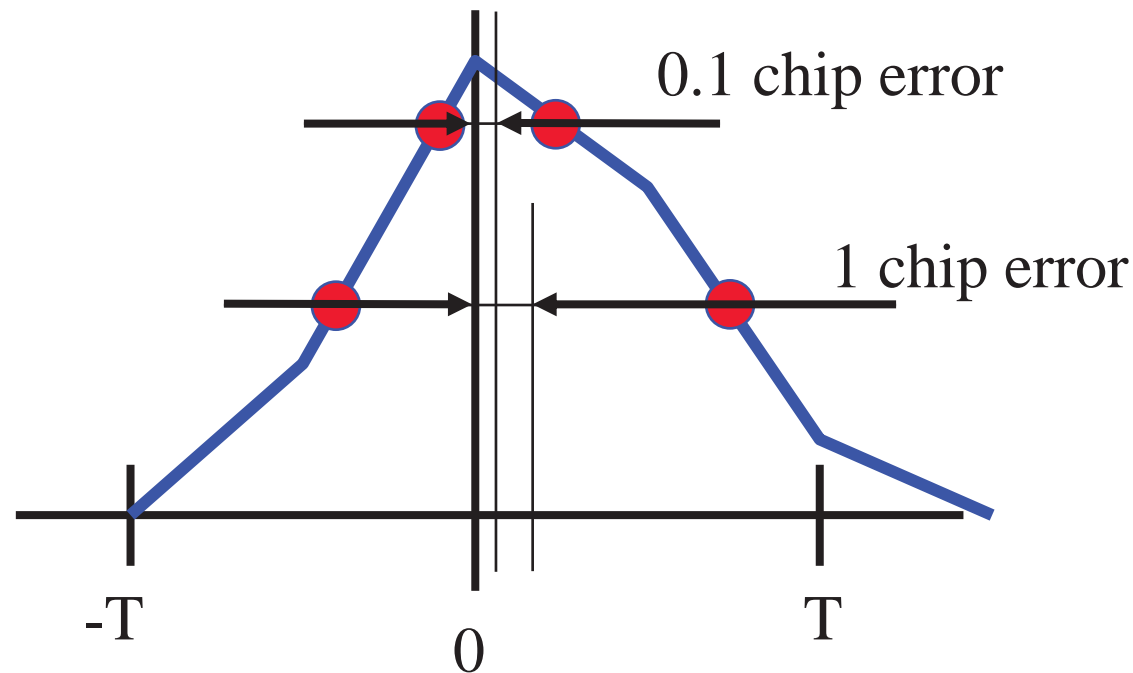


Carrier Phase Multipath Error Envelope



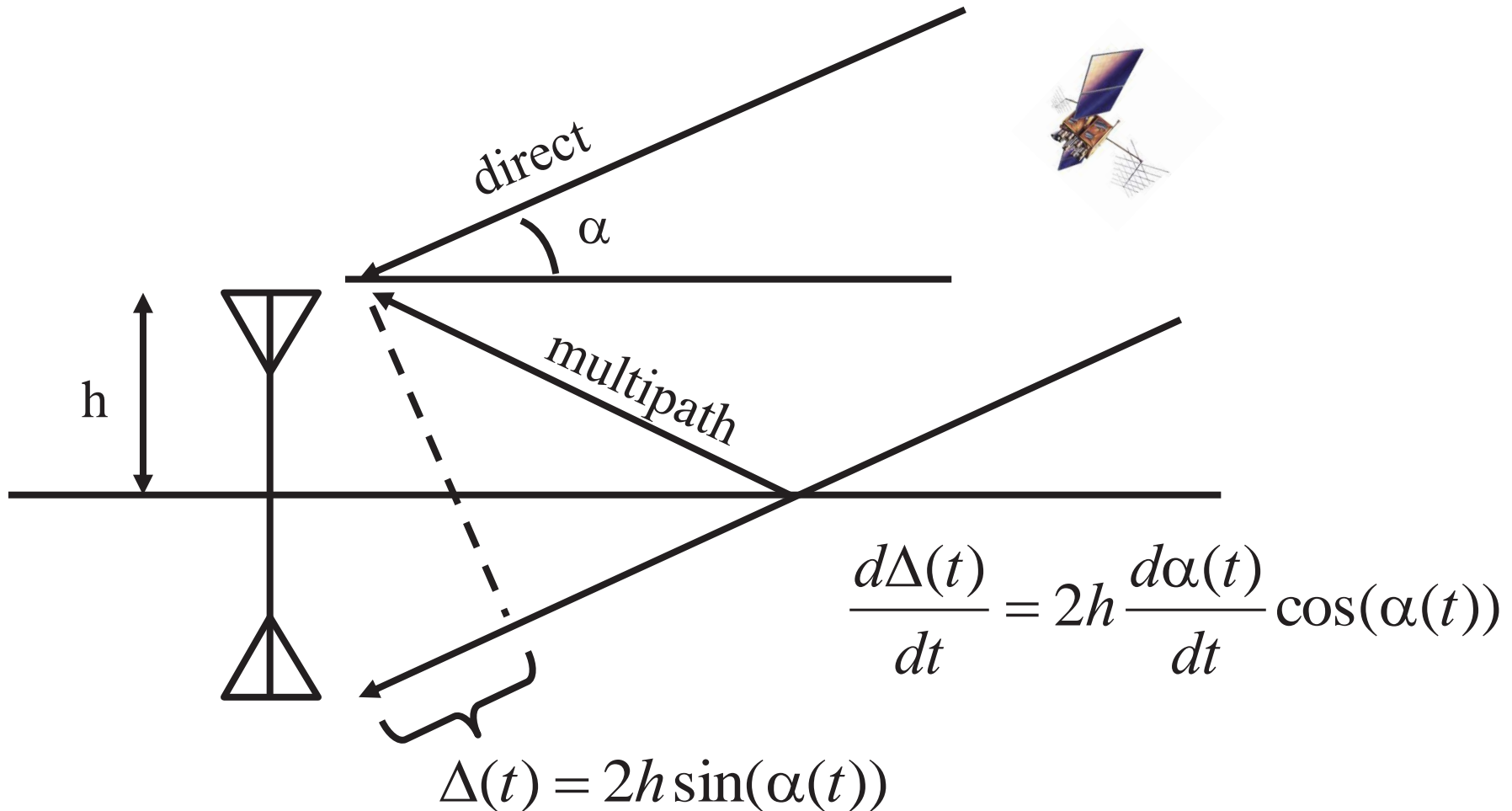
Narrow Correlator Reduces Multipath Error

Direct + Multipath Correlation Function



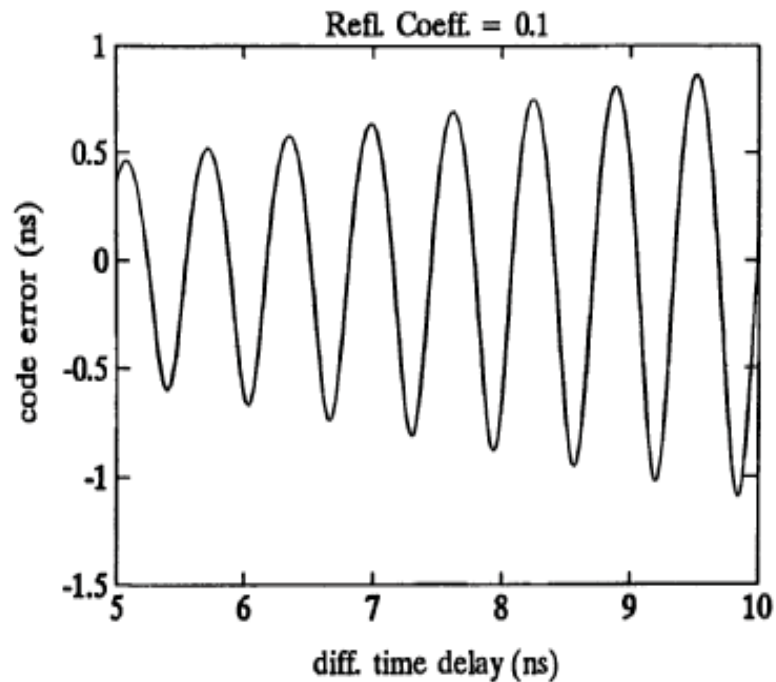
Other techniques: double delta (or edge) correlator, new waveforms BOC

Multipath Fading Frequency

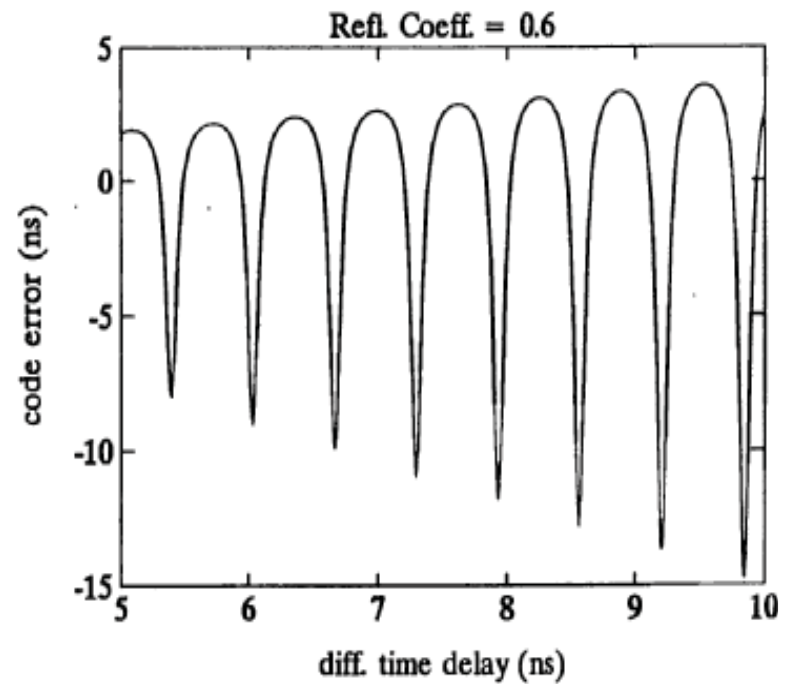


Expanded Scale Within Error Envelope

$$\alpha = 0.1$$

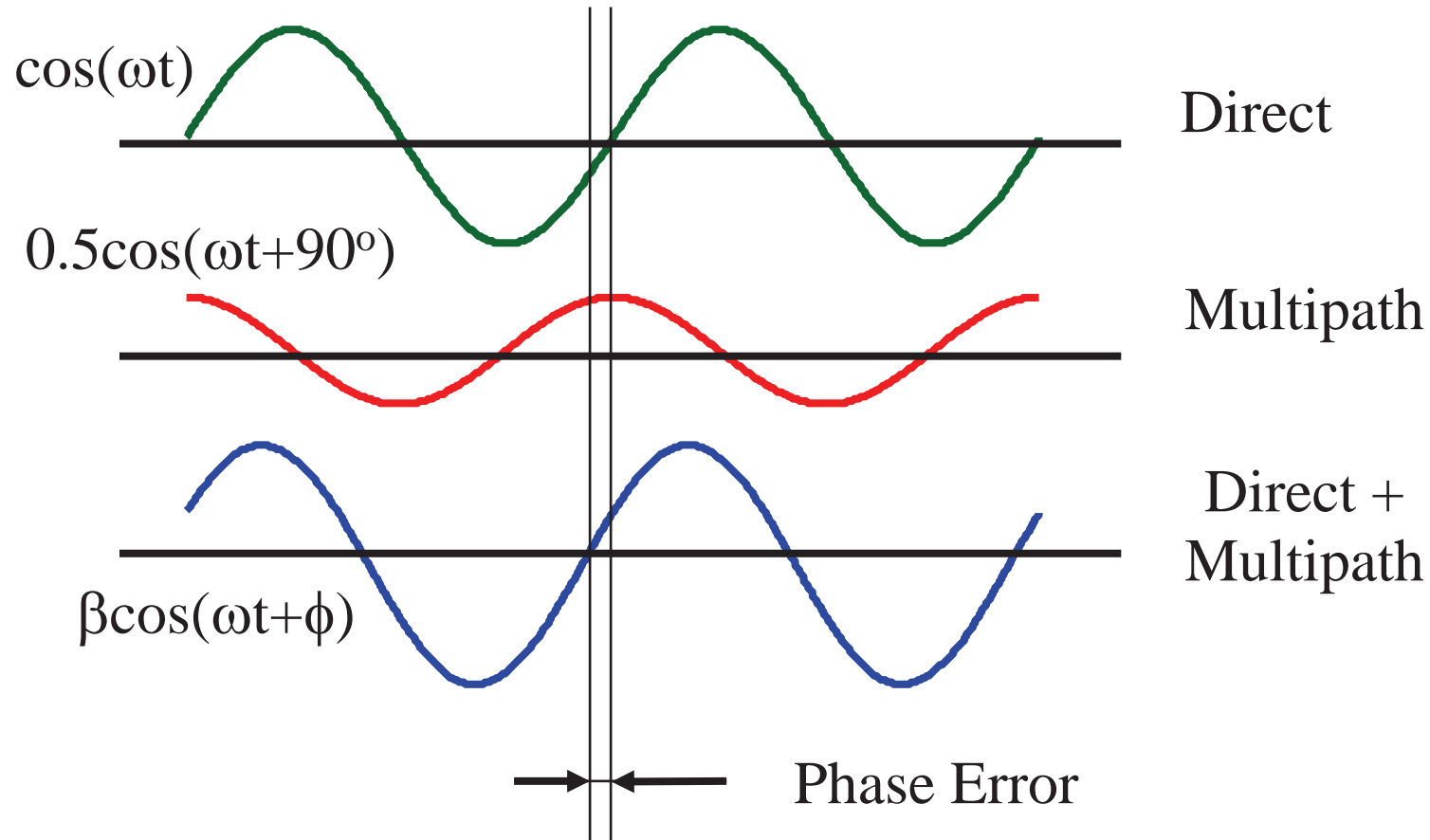


$$\alpha = 0.6$$



Error is not zero-mean !

Carrier Multipath Error Example



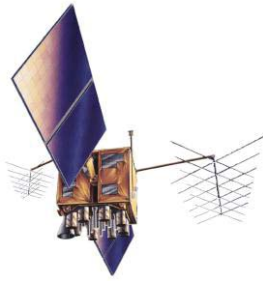
Multipath Observations

- For short multipath delays (< 10 m), errors are approximately the same for GPS P-Code and C/A-Code (0.1 – 1.0 chip correlator spacing).
- Code errors go from maximum positive to maximum negative after 0.5λ of path length difference between direct and multipath signals.
- Slow multipath fading can only occur if the reflection surface is large (reflection point must remain on the surface) and smooth relative to the GPS wavelength of 0.19 m
 - » Fading periods of 10 minutes are possible
 - » One (and only) large reflector is the ground

Some Multipath Mitigation Techniques

- Pre-Receiver
 - » Siting
 - » Antenna Design
- Receiver Processing
 - » Correlator Spacing
 - » Multipath-Estimating Delay-Lock Loop
 - » Edge Correlators
- Post-Receiver
 - » Signal-to-Noise Ratio
 - » Multiple Antennas/Receivers
 - » Repeatability/Modeling
 - » Dual-frequency Code Noise Multi-Path (CNMP) algorithm

Thermal Noise



L1 C/A-Code:
 10^{-16} W
= -160 dBW



Thermal Noise = kTB
 k = Boltzmann's constant
 T = Equivalent temperature

Tracking Loops

Carrier-to-Noise Ratio C/N_0 = Signal-to-Noise Ratio in a 1-Hz Bandwidth. For GPS: $C/N_0 > 40$ dB-Hz.

Second-Order Tracking Loops

Code Tracking (1-chip spacing)

$$\text{rms}_{\text{error}} = \Delta \sqrt{\frac{B_n}{2C/N_0}}$$

where:

Δ is the chip width;

B_n is the loop bandwidth

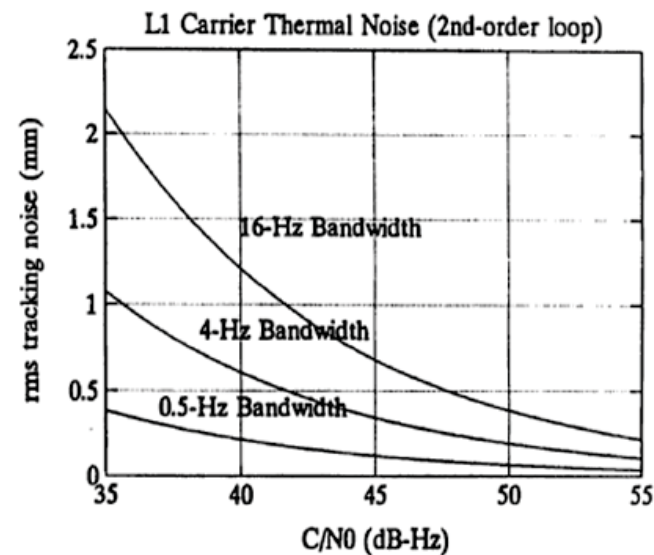
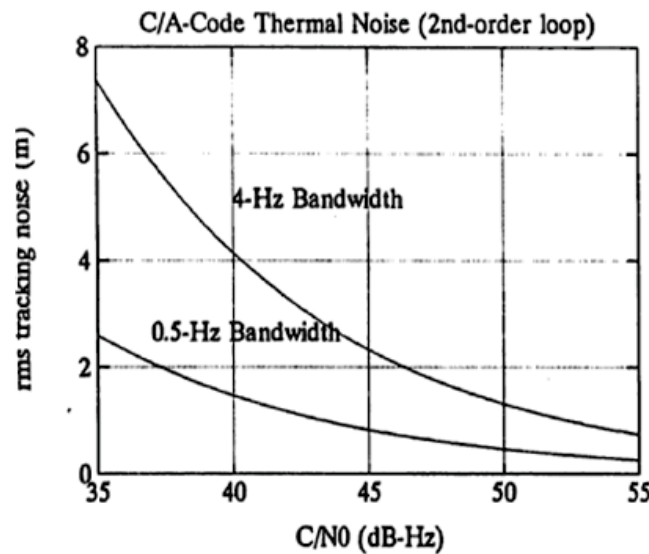
Carrier Tracking

$$\text{rms}_{\text{error}} = \frac{\lambda}{2\pi} \sqrt{\frac{B_n}{C/N_0}}$$

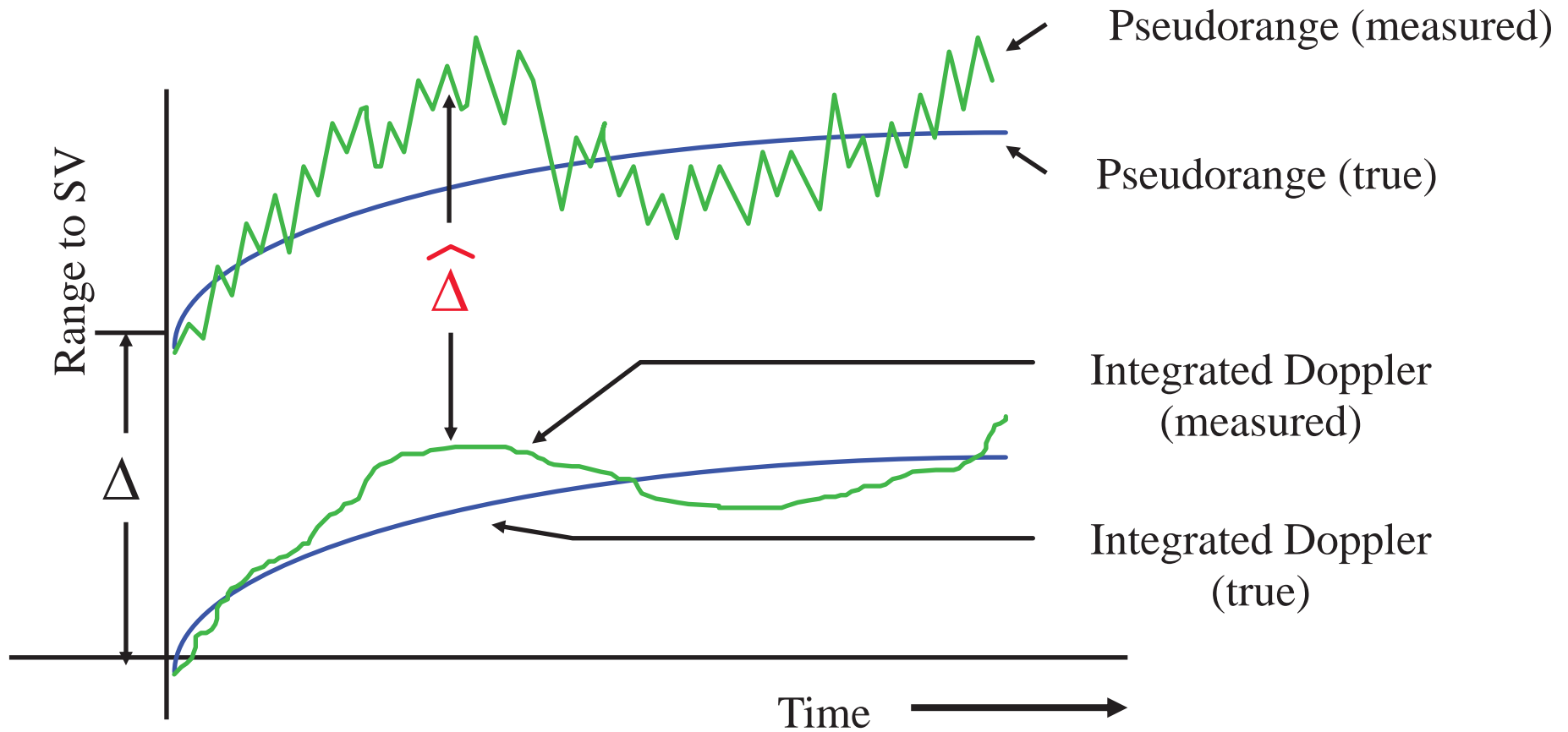
where:

λ is the wavelength

B_n is the loop bandwidth



Carrier Smoothing



Code Noise and Multipath Mitigation

ionosphere-free
pseudorange

$$\rho_{L1,corr}(t) = \rho_{L1}(t) - I_{L1}(t) =$$

$$\rho_{L1}(t) - (\rho_{L1}(t) - \rho_{L2}(t)) \frac{f_{L2}^2}{f_{L2}^2 - f_{L1}^2}$$

ionosphere-free
carrier phase

$$\phi_{L1,corr}(t) = \phi_{L1}(t) + I_{L1}(t) =$$

$$\phi_{L1}(t) - (\phi_{L2}(t) - \phi_{L1}(t)) \frac{f_{L2}^2}{f_{L2}^2 - f_{L1}^2}$$

Code-Minus-Carrier (ionosphere-free)

pseudorange noise
and multipath

$$CMC_{L1,free}(t) = \rho_{L1,corr}(t) - \phi_{L1,corr}(t)$$

$$\Delta CMC_{L1}(t) = 2.5457\tau_{PR,L1} - 1.5457\tau_{PR,L2} + 2.5457\eta_{PR,L1}(t) - 1.5457\eta_{PR,L2}(t) +$$

$$- 2.5457\tau_{AD,L1} + 1.5457\tau_{AD,L2} - 2.5457\eta_{AD,L1}(t) + 1.5457\eta_{AD,L2}(t) + B$$

CMC Processing

$$CMC_{L1,free}(t) = \rho_{L1,corr}(t) - \phi_{L1,corr}(t)$$

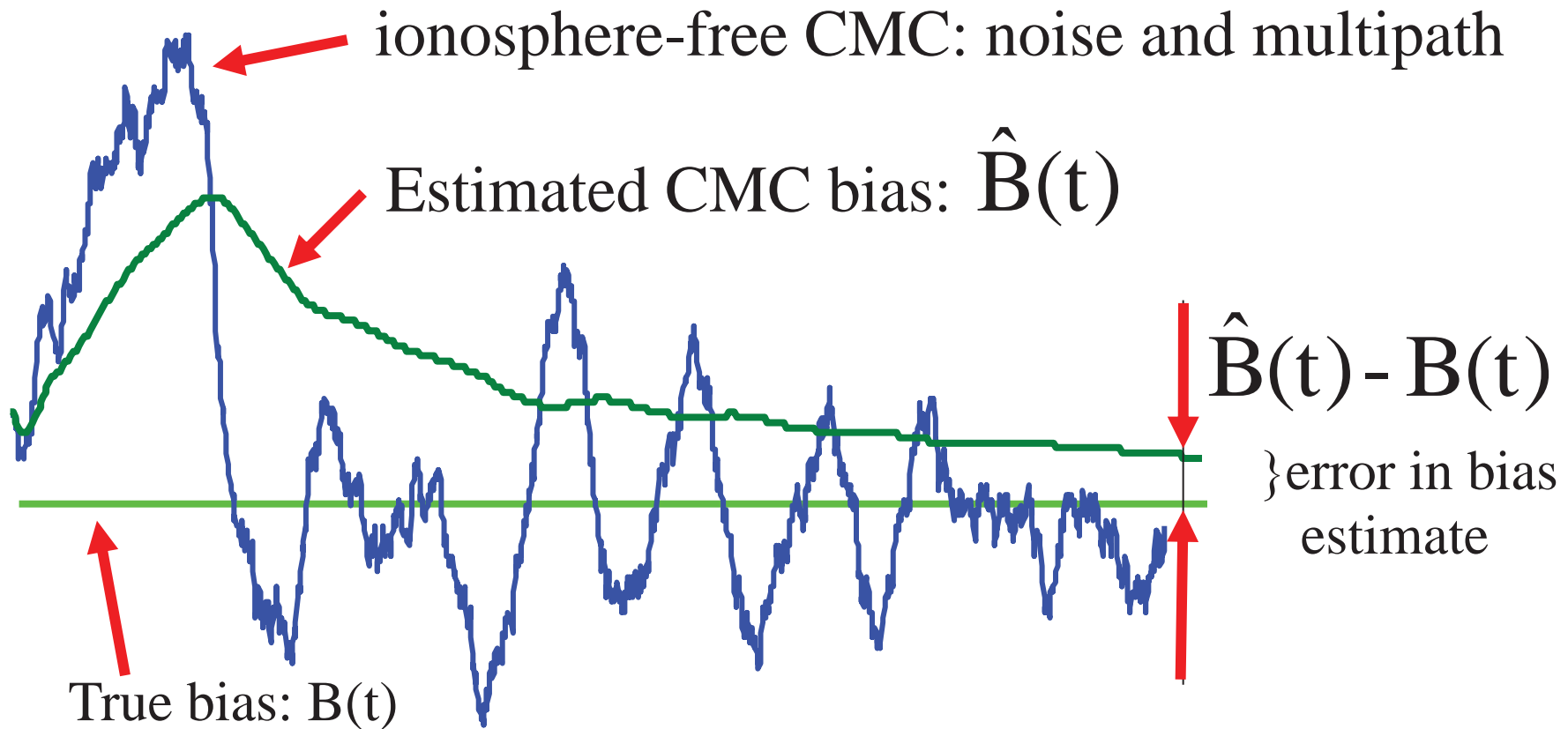
$$\Delta CMC_{L1}(t) = 2.55\tau_{PR,L1} - 1.55\tau_{PR,L2} + 2.55\eta_{PR,L1}(t) - 1.55\eta_{PR,L2}(t) + \\ - 2.55\tau_{AD,L1} + 1.55\tau_{AD,L2} - 2.55\eta_{AD,L1}(t) + 1.55\eta_{AD,L2}(t) + B$$

Thermal noise increase: $\sqrt{(2.55)^2 + (1.55)^2} \approx 3.1$

Multipath bound increase: $2.55 + 1.55 \approx 4.1$

Next step: reduce noise and multipath using Code Noise and Multi-Path (CNMP) algorithm

CNMP Algorithm Bias Estimate



Trade noise and multipath (blue curve) for a small bias

For ionospheric application, see: Ugazio, S. Van Graas, F., Pelgrum, W., Total Electron Content Measurements with Uncertainty Estimates, Proceedings of Navitec 2012, European Space Agency, 5-7 December 2012.

CNMP Algorithm

- Estimated bias (initial and after n seconds):

$$\hat{B}(0) = CMC_{L1,corr}(0)$$

$$\hat{B}(k\Delta T) = \frac{1}{n+1} \sum_{i=k-n}^k CMC_{L1,corr}(i\Delta T); \quad n = 1000$$

- Corrected pseudorange:

$$\rho_{L1,corr}(t) = \rho_{L1}(t) - CMC_{L1,corr} + \hat{B}(t)$$

- Bias bound components:

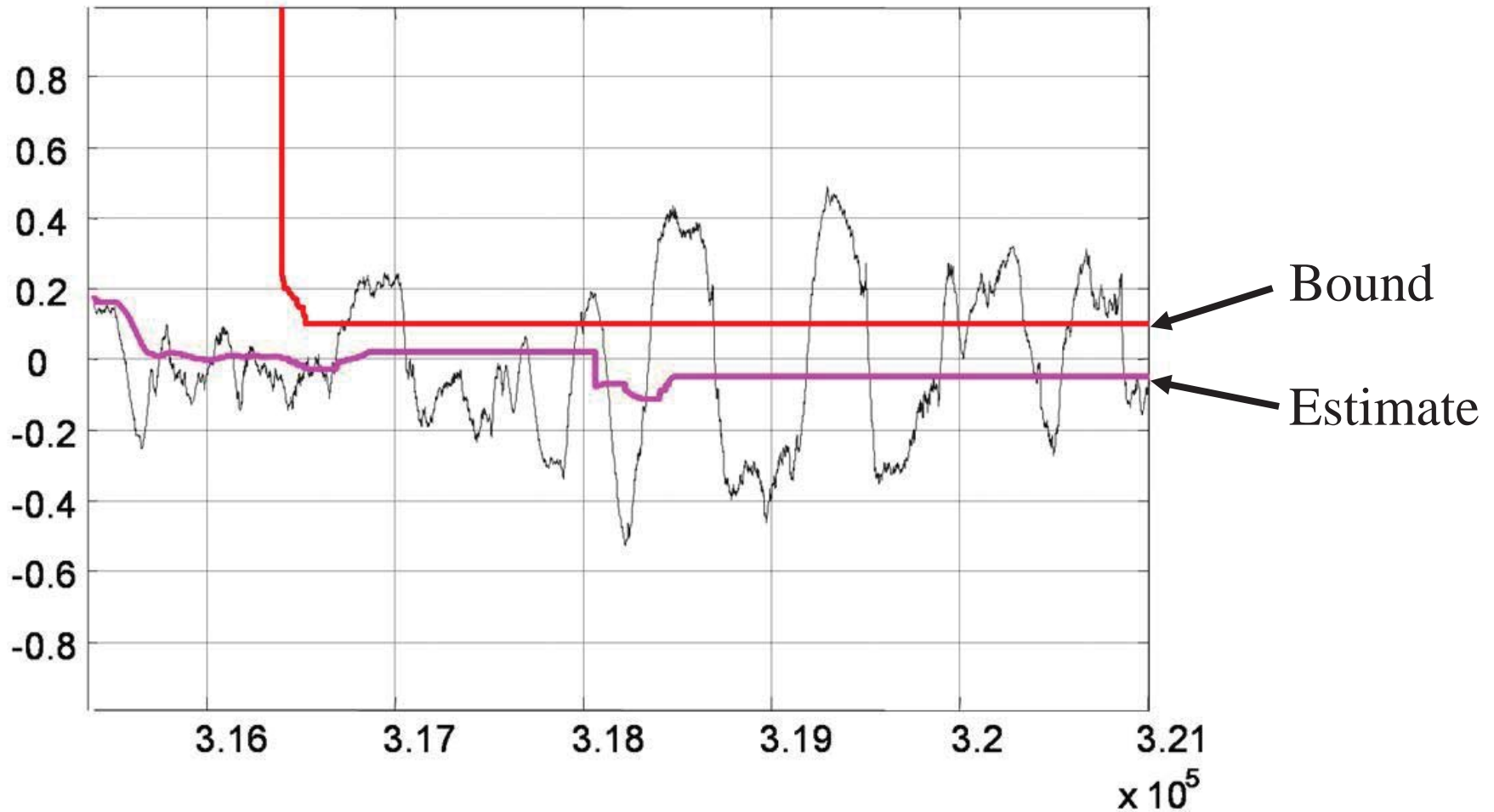
- » Peak-to-peak multipath over 1000 s

- » Antenna phase and group delays

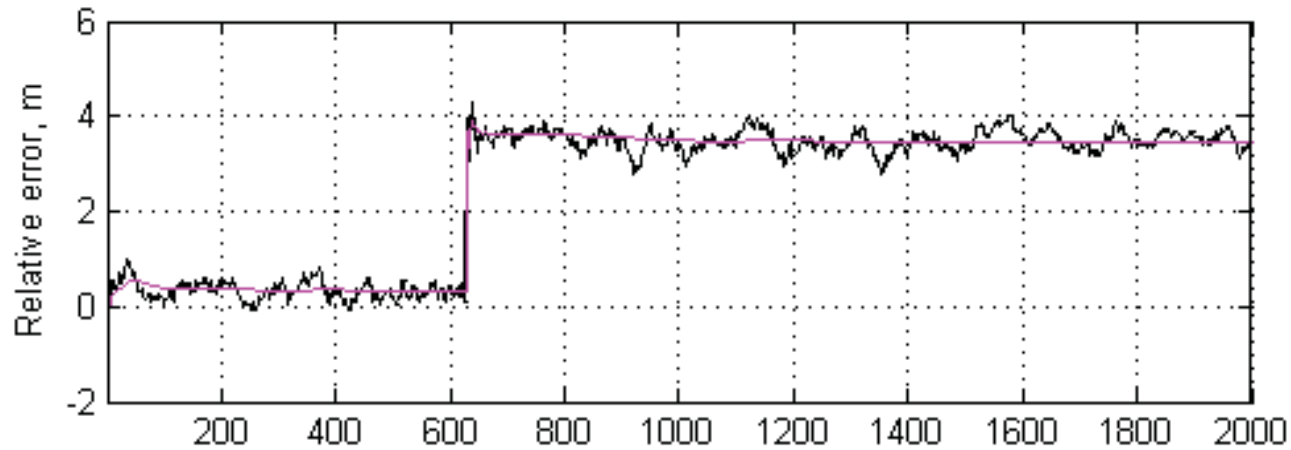
- » Code phase noise; carrier phase noise and multipath

CNMP Example Performance

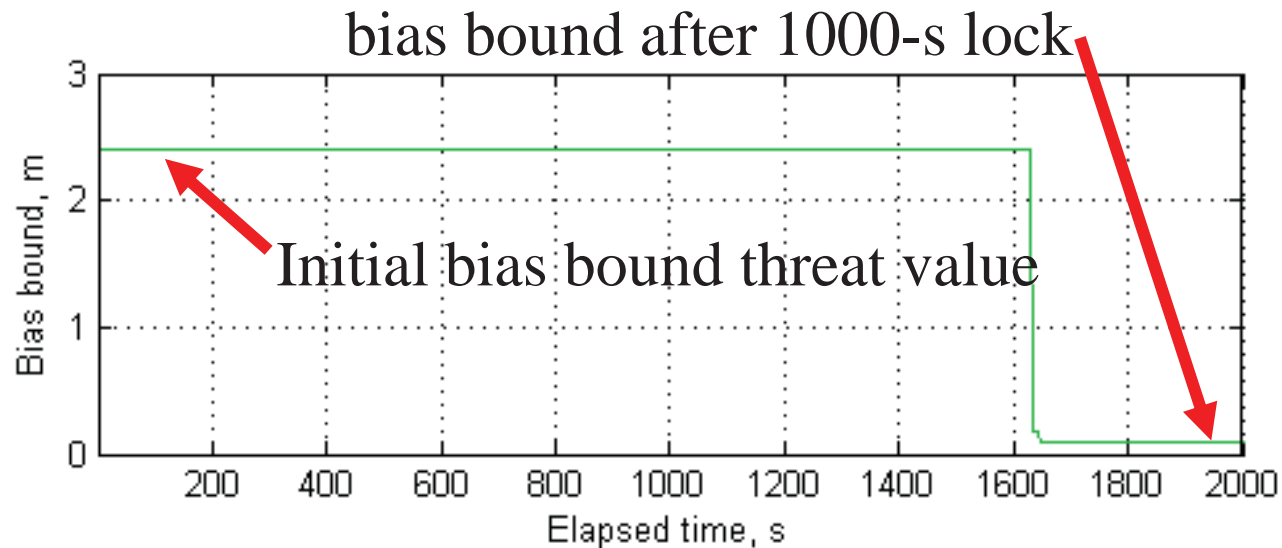
CMC for SV 19 iono corr & mean removed; MP present (k) & removed (m)



CNMP Example Performance



- Satellite 28 at reference station
- CMC raw and with averaging / filtering, relative to value at algorithm initialization



bias bound after 1000-s lock

Initial bias bound threat value

- Lock reset occurs at $t = 629$ seconds
- Bias bound shown (positive bound here; negative bound is mirror image)

GPS Pseudorange and Carrier Phase

- GPS performance continues to improve
 - » Pseudorange noise at the 0.1-m level (carrier-smoothed)
 - » Carrier phase noise at the millimeter-level
 - » Zero-age-of-data (ZAOD) ephemeris products reduce satellite orbit and clock contributions to the 0.1-m level (Precise Point Positioning)
 - Also available through Canadian Spatial Reference System CSRS (for on-line post-processing) and International GNSS Service (IGS) for near real-time processing
 - » Dual-frequency corrections with interfrequency bias compensation reduces ionospheric range delays to the 0.1-m level
 - » Tropospheric errors can be modeled to the cm-level (except during severe storm conditions – range delays of up to 1 m error, but not on all satellites)
 - » Antenna/receiver phase and group delays: phase delays can generally be calibrated to mm-level, group delays can be m-level
-

Phase and Group Delays

- Phase delay in seconds: $\tau_{phase}(\omega) = \frac{\phi(\omega)}{\omega}$
- Group delay in seconds: $\tau_{group}(\omega) = \frac{d\phi(\omega)}{d\omega}$
- If phase delay is not a function of frequency, then the group delay is zero
- Many antennas have known phase corrections (e.g. <http://www.ngs.noaa.gov/ANTCAL/>)
- Group delay corrections are more difficult to obtain:
 - » On the order of several ns for airborne antennas (azimuth and elevation angle-dependent)
 - » Time-varying for steered antennas
 - » Also introduced by receiver front-end filters (temperature sensitive, and different for each satellites and receiver)

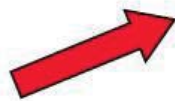
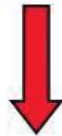
Phase Wrap-Up (known and can be corrected)

- A circularly-polarized antenna has a phase pattern that is a function of azimuth angle
- The measured phase increases by exactly 2π radians for each 360-degree rotation in azimuth $\psi(t)$:

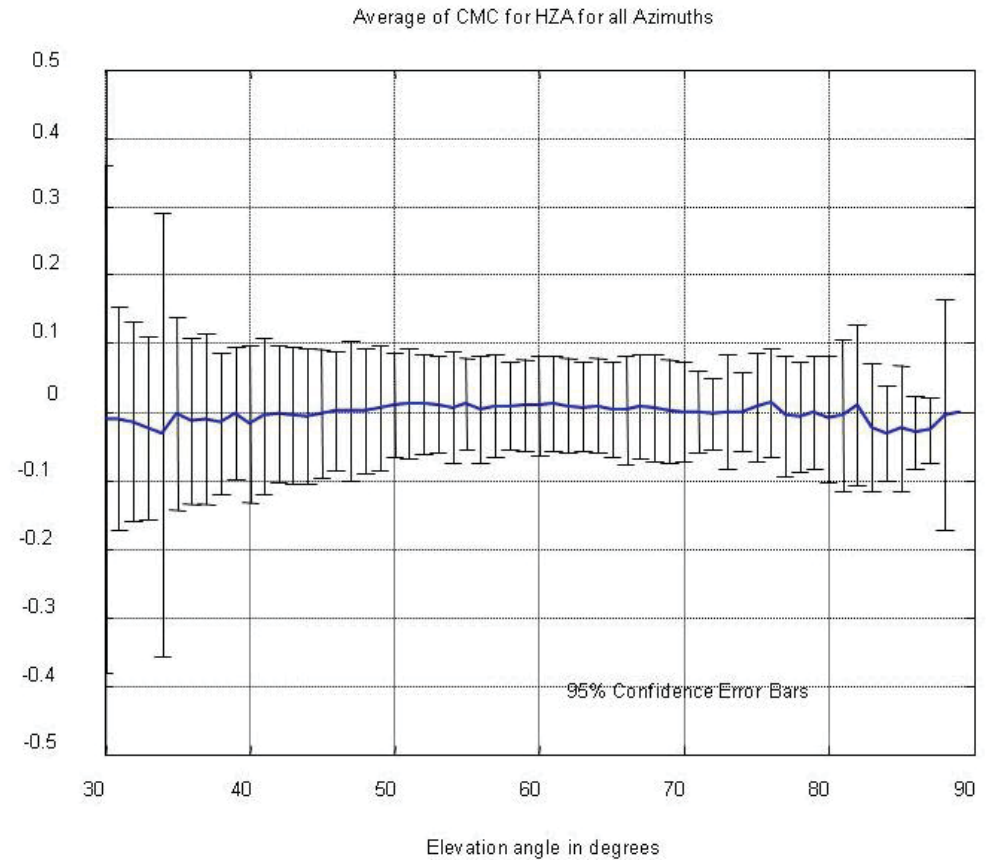
$$\phi_{wrap-up}(t) = \psi(t) \text{ (rad)}$$

- Phase increase is the same for all frequencies \rightarrow group delay is zero (pseudorange doesn't see this)
 - » Antenna rotation due to vehicle heading change: common for all satellites, creates a clock offset
 - » Satellite rotation around antenna due to orbit

High-Zenith Antenna Group Delays



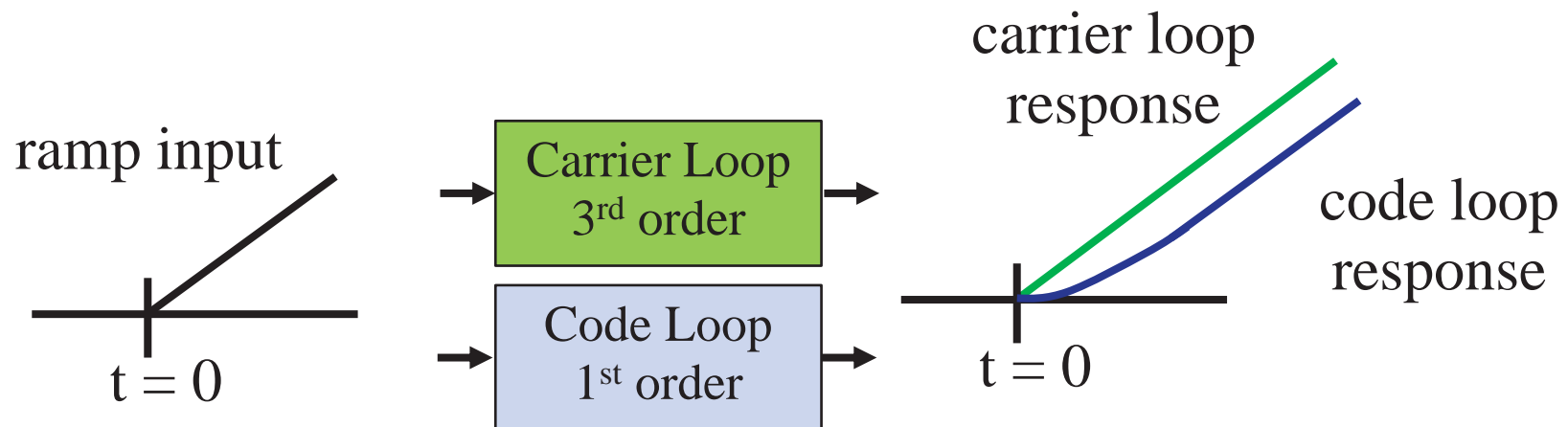
m



Van Graas, F., Bartone, C., Arthur, T., "GPS Antenna Phase and Group Delay Corrections," Proceedings of the 2004 National Technical Meeting of The Institute of Navigation, San Diego, CA, January 2004, pp. 399-408.

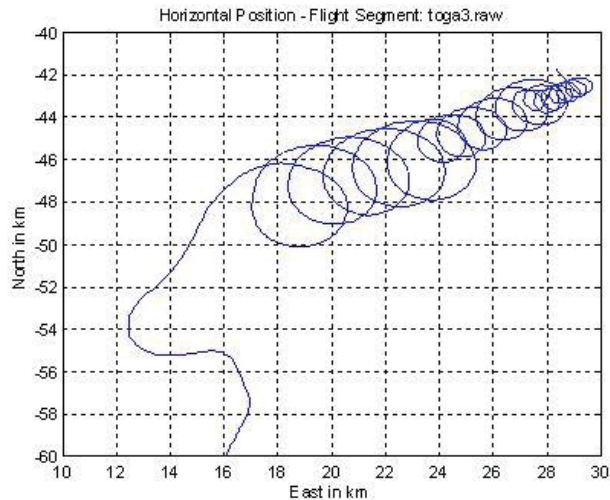
Receiver Dynamics

- Due to different code (1st-order) and carrier (3rd-order) tracking loop filters, response during dynamics is different



- Solutions
 - » Aid the code loop with the carrier loop
 - » Use same loop architectures for differential receivers

Carrier-Aided Code Tracking Loop



Piper Saratoga (N8238C)
(First arc at Henderson VOR)

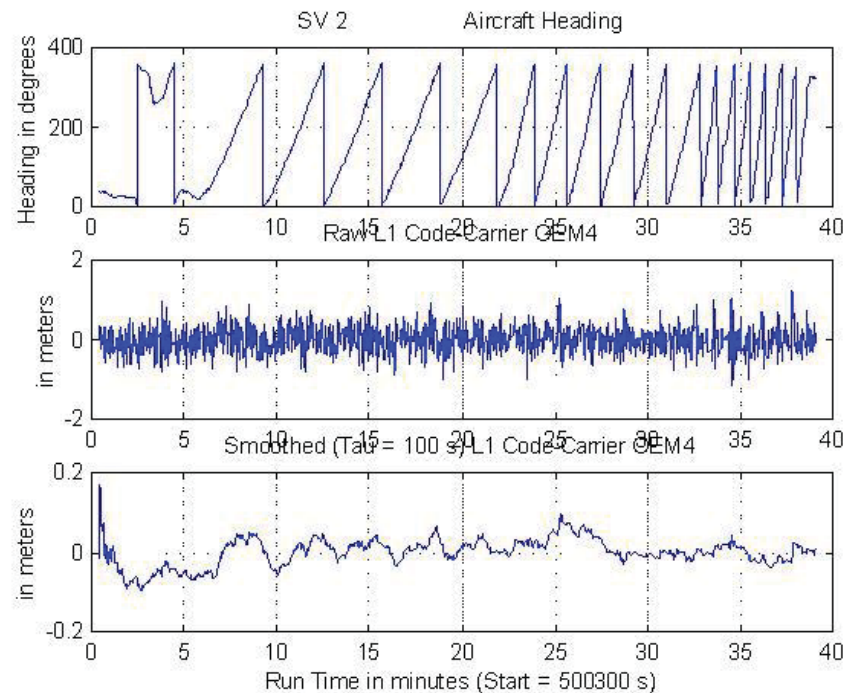


15-degree roll (1.04g - autopilot)

25-degree roll (1.1g - autopilot)

45-degree roll (1.4g - manual)

Altitude: 6,500 ft; Airspeed: 138 kts
Wind: 33 kts (200); T: 58 Fahrenheit



cm-level pseudorange residuals

Overview

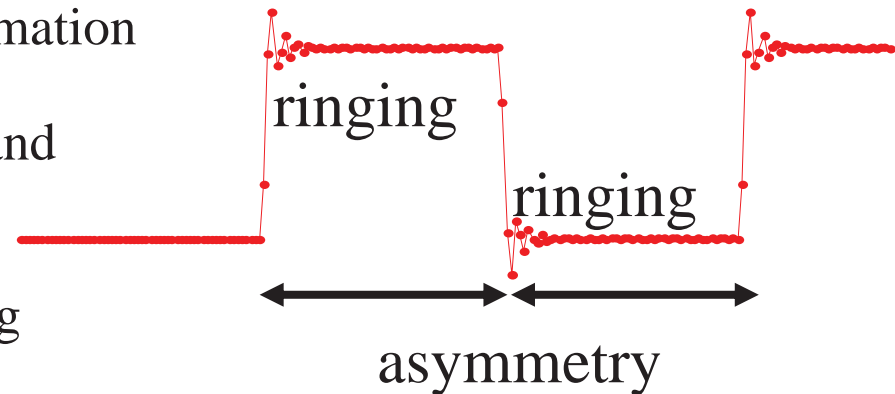
- High precision GPS techniques
 - » Relative, differential, wide area differential
 - » Kinematic, surveying, attitude determination
- GPS code and carrier phase measurements
 - » Error sources: Clock and orbit errors, ionospheric and tropospheric propagation delays, multipath, noise, antenna phase and group delays
- Additional implementation considerations

Receiver Architectures

- If using a correction network for pseudorange corrections, user receiver should use the same receiver architecture as the reference receivers; avoid "fancy" techniques
- Reason: Nominal satellite signal "malformation," also referred to as "natural deformation"

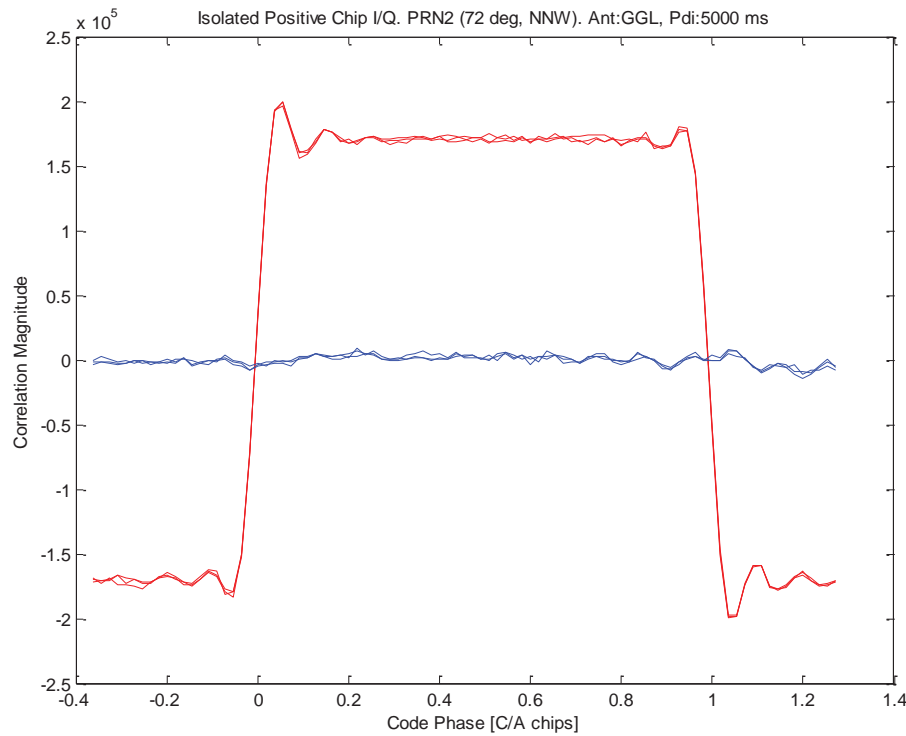
» Each satellite has a natural deformation

- Typical GBAS satellite noise and multipath: 0.1 m (1-sigma)
- Signal Deformation Monitoring allocation: 0.15 m (1 sigma)

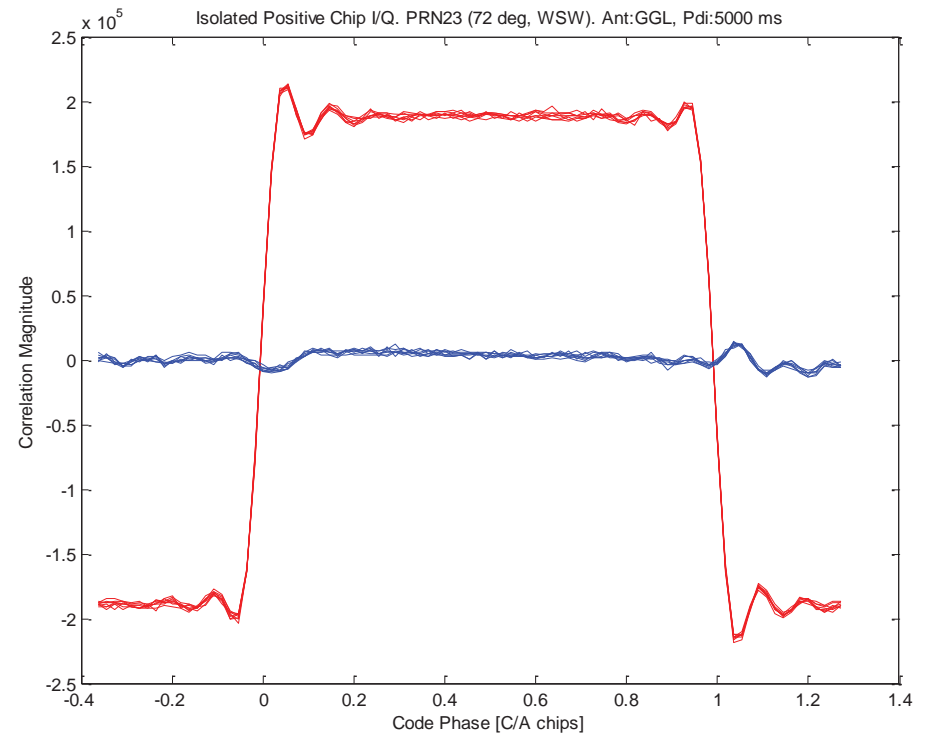


Actual Chip Shapes

PRN2



PRN23

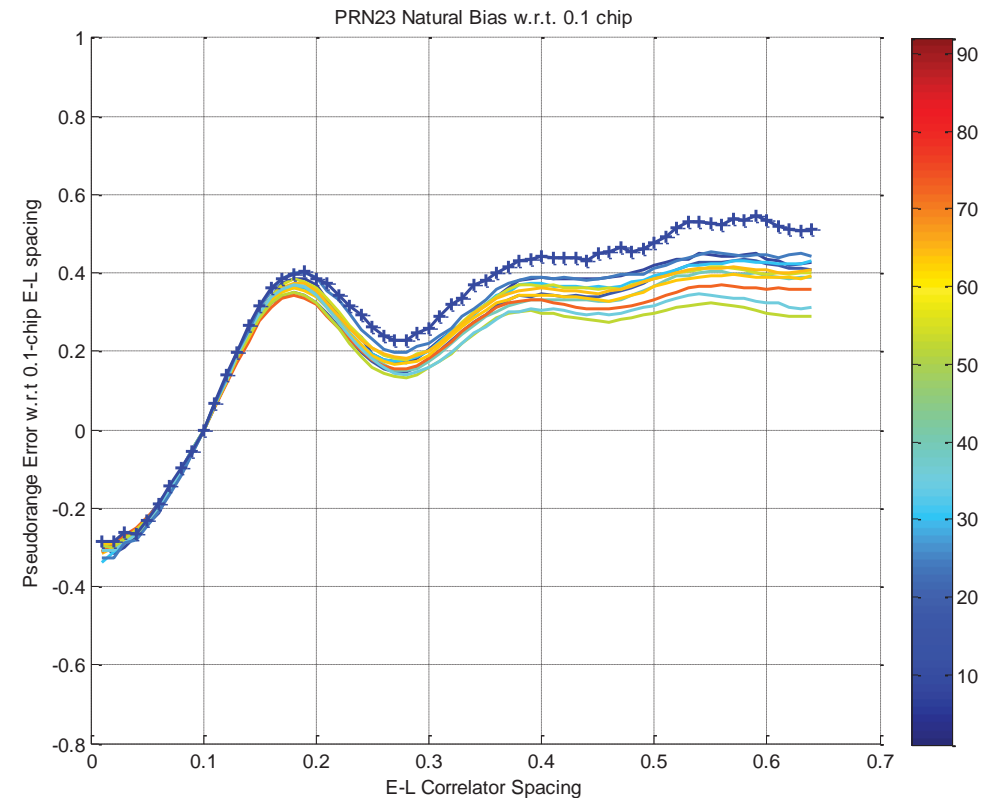
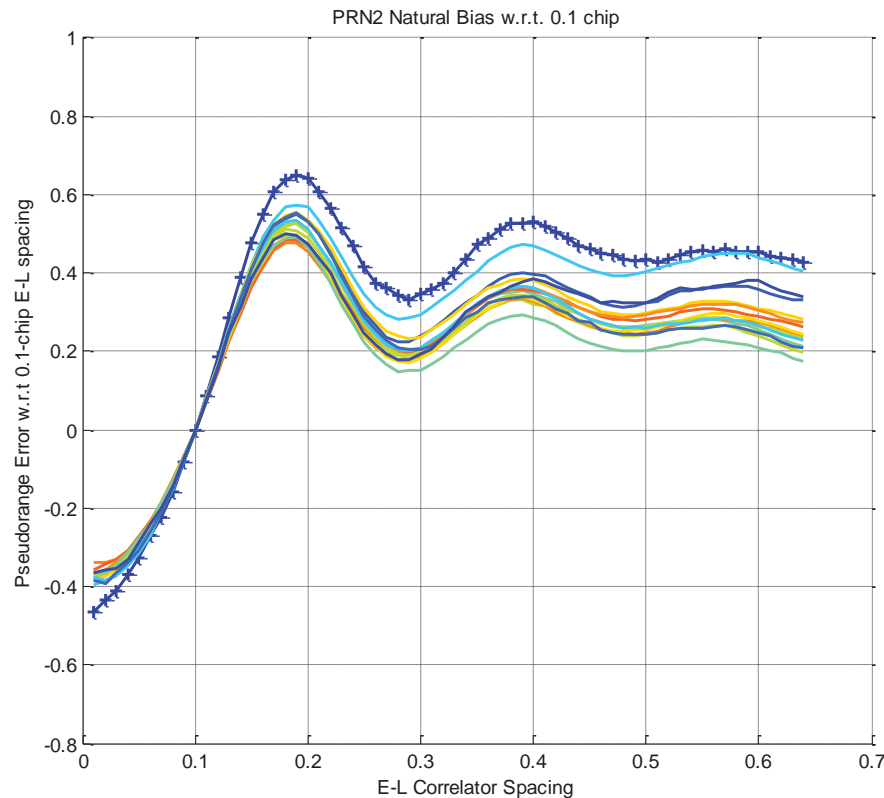


From: S. Gunawardena and F. van Graas, "High Fidelity Chip Shape Analysis of GNSS Signals using a Wideband Software Receiver," ION GNSS 2012, Nashville TN, September 18-21, 2012

Pseudorange Error wrt 0.1-chip E-L Spacing

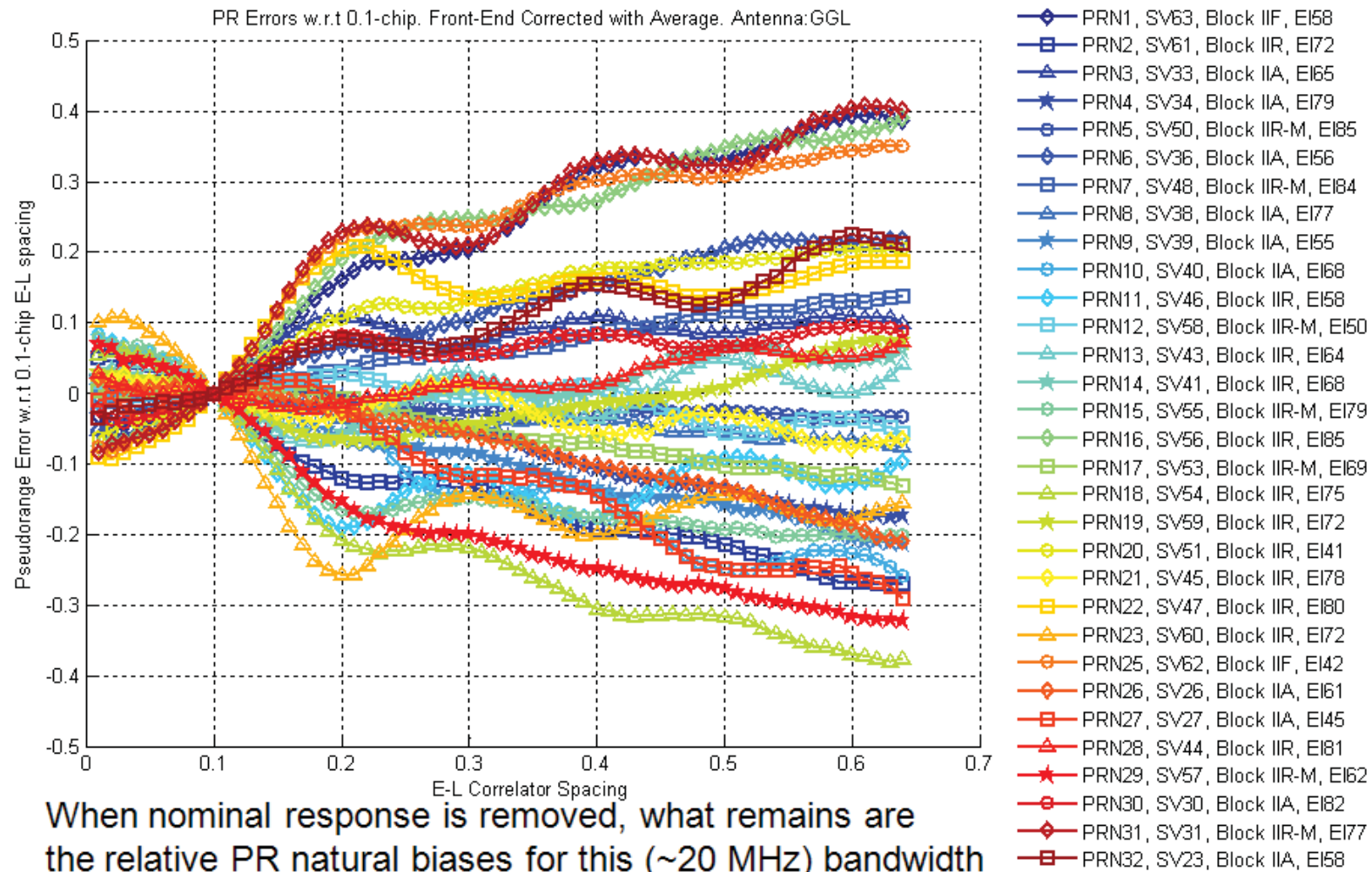
SVN61, PRN02, Block IIR

SVN60, PRN23, Block IIR



From: S. Gunawardena and F. van Graas, "Analysis of GPS Pseudorange Natural Biases using a Software Receiver," ION GNSS 2012, Nashville TN, September 18-21, 2012

Biases wrt 0.1 E-L Spacing, BW ~20 MHz



Implementation Considerations

- Receiver quality, tracking architecture, bandwidth (tracking loops: we do not only want to study the response of the tracking loops to the ionosphere, we want to study the ionosphere itself)
- Antenna installation (stability, multipath environment)
- Antenna phase (and group) delay corrections
- Local bad weather can have a significant impact on the tropospheric delays
- Differential/Relative: Source of correction data
 - » Error approaches zero as user approaches the reference site
- Initialization time (re-start time)
 - » Additional reliance on carrier phase reduces the robustness of the solution, but improves accuracy
- Integrity: so far only LAAS (GBAS) and WAAS (SBAS) are proven safe for aircraft precision approach
 - » Carrier-smoothed code architectures
- More satellites → better carrier phase solution performance